Brain Structure and Function (2020) 225:249–284
https://doi.org/10.1007/s00429-019-01999-2

ORIGINAL ARTICLE

Cholecystokinin in the central nervous system of the sea lamprey *Petromyzon marinus*: precursor identification and neuroanatomical relationships with other neuronal signalling systems

D. Sobrido-Cameán[1] · L. A. Yáñez-Guerra[2] · D. Robledo[3] · E. López-Varela[1] · M. C. Rodicio[1] · M. R. Elphick[2] · R. Anadón[1] · Antón Barreiro-Iglesias[1]

Received: 6 May 2019 / Accepted: 27 November 2019 / Published online: 5 December 2019

Abstract

Cholecystokinin (CCK) is a neuropeptide that modulates processes such as digestion, satiety, and anxiety. CCK-type peptides have been characterized in jawed vertebrates and invertebrates, but little is known about CCK-type signalling in the most ancient group of vertebrates, the agnathans. Here, we have cloned and sequenced a cDNA encoding a sea lamprey (*Petromyzon marinus* L.) CCK-type precursor (*PmCCK*), which contains a CCK-type octapeptide sequence (PmCCK-8) that is highly similar to gnathostome CCKs. Using mRNA in situ hybridization, the distribution of *PmCCK*-expressing neurons was mapped in the CNS of *P. marinus*. This revealed *PmCCK*-expressing neurons in the hypothalamus, posterior tubercle, prethalamus, nucleus of the medial longitudinal fasciculus, midbrain tegmentum, isthmus, rhombencephalic reticular formation, and the putative nucleus of the solitary tract. Some *PmCCK*-expressing neuronal populations were only observed in adults, revealing important differences with larvae. We generated an antiserum to PmCCK-8 to enable immunohistochemical analysis of CCK expression, which revealed that GABA or glutamate, but not serotonin, tyrosine hydroxylase or neuropeptide Y, is co-expressed in some PmCCK-8-immunoreactive (ir) neurons. Importantly, this is the first demonstration of co-localization of GABA and CCK in neurons of a non-mammalian vertebrate. We also characterized extensive cholecystokinergic fibre systems of the CNS, including innervation of habenular subnuclei. A conspicuous PmCCK-8-ir tract ascending in the lateral rhombencephalon selectively innervates a glutamatergic population in the dorsal isthmic grey. Interestingly, this tract is reminiscent of the secondary gustatory/visceral tract of teleosts. In conclusion, this study provides important new information on the evolution of the cholecystokinergic system in vertebrates.

Keywords Lamprey · Cholecystokinin · GABA · Glutamate · Brain · Spinal cord

Abbreviations

5-HT	Serotonin
ALL	Anterior lateral line nerve
ARRN	Anterior rhombencephalic reticular nucleus
B3	Rhombencephalic Müller cell 3
Ch	Optic chiasm
dc	Dorsal cell
DC	Dorsal column
DCN	Dorsal column nucleus
DHyp	Dorsal hypothalamus
dic	Dorsal isthmic commissure
DIG	Dorsal isthmic grey
DN	Dorsal nucleus of the octavolateralis area
dV	Descending trigeminal root
Em	Prethalamic eminence
fr	Fasciculus retroflexus
GABA	Gamma-aminobutyric acid

Electronic supplementary material The online version of this article (https://doi.org/10.1007/s00429-019-01999-2) contains supplementary material, which is available to authorized users.

✉ Antón Barreiro-Iglesias
anton.barreiro@usc.es

[1] Department of Functional Biology, Edificio CIBUS, Campus Vida, Faculty of Biology, Universidade de Santiago de Compostela, 15782 Santiago de Compostela, A Coruña, Spain

[2] School of Biological and Chemical Sciences, Queen Mary University of London, Mile End Road, London E1 4NS, UK

[3] The Roslin Institute and Royal (Dick) School of Veterinary Studies, The University of Edinburgh, Midlothian EH25 9RG, UK

Gl	Glomerular layer of olfactory bulb
Ha	Habenula
NH	Neurohypophysis
Hyp	Hypothalamus
I1	Giant isthmic neuron
IIId	Oculomotor nucleus, dorsal subnucleus
III-l	Oculomotor nucleus, lateral subnucleus
IP	Interpeduncular nucleus
IS	Isthmus
ISd	Dorsal isthmus region
ISv	Ventral isthmus region
IV	Trochlear nucleus
IXm	Glossopharyngeal motor nucleus
lHa	Left habenula
LHyp	Lateral hypothalamus
LP	Lateral pallium
LPd	Lateral pallium, dorsal part
LPv	Lateral pallium, ventral part
LT	Lamina terminalis
M	Mesencephalon
M1–3	Giant Müller cells 1–3
M5	Nucleus M5 of Schober
Ma	Mammillary nucleus
mlf	Medial longitudinal fasciculus
MN	Medial nucleus of the octavolateralis area
MP	Medial pallium
Mr	Mammillary recess
MRRN	Medial rhombencephalic reticular nucleus
Mth	Mauthner neuron
NH	Neurohypophysis
Nmlf	Nucleus of the medial longitudinal fasciculus
OB	Olfactory bulb
OLA	Octavolateralis area
OMa	Octavomotor anterior nucleus
ON	Optic nerve
OT	Optic tectum
ot	Optic tract
P	Pineal organ
PC	Posterior commissure
pl	Choroid plexus
PLL	Posterior lateral line nerve
Pm	*Petromyzon marinus*
PO	Preoptic nucleus
PoC	Nucleus of the postoptic commissure
PoR	Postoptic recess
prIII	Perioculomotor region
PRRN	Posterior rhombencephalic reticular nucleus
PT	Pretectum
PTh	Prethalamus
PTN	Posterior tubercle nucleus
Rh	Rhombencephalon
rHa	Right habenula
N-SC	Neurobiotin labelling from the spinal cord
NPY	Neuropeptide Y
SC	Spinal cord
ShL	Subhippocampal lobe
sl	Sulcus limitans
So	Nucleus of the solitary tract
SOC	Spino-occipital motor column
Sp	Septum
Str	Striatum
TH	Tyrosine hydroxylase
Th	Thalamus
TS	Torus semicircularis
v	Ventricle
VIIm	Facial motor nucleus
VIII	Octaval nerve
VHyp	Ventral hypothalamus
Vm	Trigeminal motor nucleus
VN	Ventral nucleus of the octavolateralis area
Vs	Trigeminal spinal nucleus
Xm	Vagal motor nucleus
zl	Zona limitans intrathalamica

Introduction

Cholecystokinin (CCK) is a peptide of the gastrin/cholecystokinin family that was originally isolated from jejunal extracts as a gastrointestinal hormone that induced gallbladder contraction (Ivy and Oldberg 1928; Rehfeld 2017). A component of pig intestine extracts, originally known as pancreozymin (stimulates secretion of pancreatic enzymes), also exhibited CCK-type activity causing gallbladder contraction. In 1962, a 33-amino acid peptide isolated from pig intestines was reported to activate both gallbladder contractions (CCK action) and pancreatic enzyme secretion (pancreozymin action), and the sequence of porcine CCK/pancreozymin was determined in 1968 (Mutt and Jorpes 1968). Subsequent studies have revealed that CCK also regulates feeding behaviour by mediating mechanisms of satiety (Rehfeld 2017). Furthermore, CCK is widely distributed in the central and peripheral nervous system (Larson and Rehfeld 1979) and in several endocrine glands (Hansen 2001; Rehfeld 2017) of mammals.

Genes encoding the rat, human, and mouse CCK have been sequenced (Deschenes et al. 1985; Takahashi et al. 1986; Vitale et al. 1991). In these species, the CCK transcriptional unit is about 7 kilobases in length, is interrupted by several introns (Hansen 2001), and encodes a 115 amino acid precursor CCK. This precursor protein comprises an N-terminal signal peptide and is cleaved by proteases to liberate mature peptide fragments of various lengths (CCK-58 to CCK-5) that share a C-terminal bioactive GWMDFamide sequence. Furthermore, an important feature of CCK-type peptides is the presence of a sulfated tyrosine at the seventh

amino acid residue from the C-terminus (Rehfeld 2017). The major isoform of CCK in the brain is sulfated CCK-8 (Agersnap et al. 2016).

Another member of the gastrin/CCK family present in mammals and other jawed vertebrates is gastrin (Roelants et al. 2010), which shares a C-terminal tetrapeptide with CCK and has an O-sulfated tyrosine (Rehfeld 2017). The gastrin-CCK family also includes the peptide cionin in the invertebrate chordate *Ciona intestinalis* (Conlon et al. 1988; Monstein et al. 1993) and the frog skin venoms caerulein and phyllocaerulein, all of which share the same C-terminal amidated tetrapeptide sequence and sulfated tyrosines (Roelants et al. 2010; Rehfeld 2017). CCK-type neuropeptide precursors have been identified in deuterostomian invertebrates (starfish, sea urchin, acorn worm: Semmens et al. 2016) and CCK-type peptides known as sulfakinins have been identified in insects and other arthropods (Nachman et al. 1986a, b). Interestingly, CCK-type peptides and receptors appear to have been lost in cephalochordates (Mirabeau and Joly 2013).

The distribution of CCK-expressing neurons in the mammalian CNS has been thoroughly studied using antibodies raised against CCK (Larson and Rehfeld 1979; Hökfelt et al. 1980; Dockray 1980; Vanderhaeghen et al. 1980; Kubota et al. 1983; Cho et al. 1983; Fox et al. 1991) and with mRNA in situ hybridization (ISH) (Burgunder and Young 1989a, b, 1990a, b; De Belleroche et al. 1990; Jayaraman et al. 1990; Hermanson et al. 1998). In rats, CCK immunoreactivity is present in numerous cells distributed in the olfactory bulb, cortex, hippocampus, amygdala, preoptic region, hypothalamus, thalamus, midbrain tegmentum, inferior colliculus, and some hindbrain nuclei (Vanderhaeghen et al. 1980; Kubota et al. 1983; Tohyama and Takatsuji 1998). Moreover, studies on the rat brain indicate that CCK is a neurotransmitter/neuromodulator with a variety of functions that include regulation of feeding (satiety), locomotion, self-stimulation, anxiety, and learning and memory (for review, see Morley 1982; Rehfeld 2017). CCK exerts its effects via two G-protein coupled receptors (CCKAR and CCKBR) that exhibit differential distribution in the CNS: both receptor types are expressed in the cortex, olfactory regions, hippocampal formation, septum, and interpeduncular nucleus, whereas the medial preoptic area and some hypothalamic nuclei (paraventricular nucleus and arcuate nucleus) only express CCKAR, and most amygdaloid nuclei only express CCKBR (Honda et al. 1993; Bowers and Ressler 2015). CCKAR and CCKBR signalling appear to act synergistically during development (Nishimura et al. 2015).

The family of CCK/gastrin-type peptides has also been characterized by biochemical assays and gene sequencing in most non-mammalian vertebrate groups (Johnsen et al. 1997; Roelants et al. 2010; Dupré and Tostivint 2014). In elasmobranchs, both peptides (gastrin and CCK) are present, and their genes have been cloned, indicating that these two related genes evolved by gene duplication more than 500 million years ago (Johnsen et al. 1997; Roelants et al. 2010). Moreover, CCK is mainly expressed in the brain of elasmobranchs (MacDonald and Volkoff 2009a, b; Dupré and Tostivint 2014). In teleosts, gastrin and two or three CCK genes have been cloned and several studies have shown that CCK genes are expressed in the brain (see Jensen et al. 2001; Kurokawa et al. 2003; Murashita et al. 2009). The distribution of cholecystokinergic neurons in the brain of non-mammalian vertebrates has been mainly studied by immunohistochemistry with antibodies raised against mammalian CCKs (lampreys: Brodin et al. 1988; teleosts: Batten et al. 1990; Moons et al. 1992; frog: Petkó and Kovács 1996) or by ISH (birds: Maekawa et al. 2007; Lovell and Mello 2011; Atoji and Karim 2014). Investigations of CCK function in fishes have reported changes in CCK mRNA expression between fasting and feeding, or changes in feeding behaviour after administration of CCK (Volkoff et al. 2005; Murashita et al. 2009; MacDonald and Volkoff 2009a, 2009b).

CCK-type peptides have been studied in lampreys since the early 1970s. Extracts of lamprey gut have secretin-like and pancreozymin-like actions on the rat pancreas (Barrington and Dockray 1970) and these extracts also cross-react with antisera specific for the C-terminus of mammalian gastrin or CCK (Dockray 1977). Holmquist et al. (1979) used chromatographic techniques and radioimmunoassay with antisera specific for different regions of mammalian gastrin and CCK to investigate the properties of CCK-like peptides in lampreys. In both the brain and intestine, two factors that cross-react with antisera specific for gastrin or CCK were detected. In the gut epithelium of lampreys, gastrin/CCK-like immunoreactivity was observed in flask-shaped endocrine cells (Van Noorden and Pearse 1974; Brodin et al. 1988; Yui et al. 1988).

The presence of CCK-like peptides in brain extracts of lampreys (*Lampetra tridentata* and *Lampetra fluviatilis*) was first reported by Holmquist et al. (1979). Shortly after, the presence of CCK-like-ir neurons and fibres was reported in the lamprey spinal cord (van Dongen et al. 1985; Buchanan et al. 1987), and then in the brain (Ohta et al. 1988; Brodin et al. 1988). The origin of some CCK-like-ir spinal cord fibres has been traced to CCK-like-ir reticulospinal neurons in the posterior rhombencephalic reticular nucleus (Ohta et al. 1988; Brodin et al. 1988). The distribution of CCK-like-ir neurons in the lamprey spinal cord and brain (in the middle rhombencephalic reticular nucleus, the reticular nucleus of the mesencephalon, and the hypothalamus) was investigated using anti-mammalian CCK antisera with different properties (Brodin et al. 1988). In the spinal cord, three separate CCK-like systems were revealed: a ventral and lateral fibre system arising from neurons in the posterior rhombencephalic reticular nucleus, a dorsal

root–dorsal column system of fibres originating from cells in the dorsal root ganglia, and an intraspinal system of CCK/serotonin (5-HT)-positive neurons located below the central canal, with the latter two systems probably non-specifically labelled by some of the CCK antisera. Furthermore, in the retina of *Lampetra japonica,* CCK-ir fibres, but not perikarya, are present in the inner plexiform layer (Negishi et al. 1986).

Lampreys are extant relatives of the earliest group of vertebrates, the agnathans, which diverged from the rest of vertebrates more than 450 million years ago. During the life cycle of lampreys, large changes in lifestyle and feeding behaviour are reflected in differences in the relative size of the major brain subdivisions and digestive organs (see Salas et al. 2015). With the aim to further contribute to our knowledge of the evolution and development of the cholecystokinergic system in vertebrates, here, we have cloned and sequenced a cDNA encoding the sea lamprey *Petromyzon marinus* CCK precursor (*PmCCK*). This then enabled analysis of the expression of *PmCCK* in the brain and spinal cord of larval and adult lampreys using ISH. The predicted sequence of the mature CCK-8 peptide of the sea lamprey (PmCCK-8) was determined and an antibody specific for the sulfated version of PmCCK-8 was generated. Then, the anti-PmCCK-8 antiserum was used to characterize the distribution of immunoreactive cells and fibres in the central nervous system of larvae and adults. PmCCK-8 immunohistochemistry was combined with immunohistochemical labelling of neurotransmitters (glutamate, GABA, 5-HT), the catecholamine-synthesizing enzyme tyrosine hydroxylase (TH), and the orexigenic peptide neuropeptide Y (NPY) or with tract-tracing from the spinal cord. This study provides the first identification of a CCK-type precursor in a jawless vertebrate and an extensive anatomical characterization of the cholecystokinergic system in the sea lamprey CNS, including the occurrence of notable differences between larvae and adults.

Materials and methods

Animals

Larval ($n = 31$), downstream migrating young adult (post-metamorphic juveniles; $n = 10$) and upstream-migrating adult ($n = 6$) sea lampreys, *P. marinus*, were used for this study (see Table 1 for details on the animals used in each of the experiments). Downstream migrating young adults and larvae (ammocoete: lengths comprised between 80 and 110 mm, 4–7 years old) were collected from the River Ulla (Galicia, Spain) with permission from the *Xunta de Galicia*. Upstream-migrating adults were acquired from local suppliers. Adults were fixed freshly, and larvae were maintained in aquaria containing river sediment and with appropriate feeding, aeration, and temperature conditions until the day of use. Before all experiments, animals were deeply anesthetized with 0.1% tricaine methanesulfonate (MS-222; Sigma-Aldrich, St. Louis, MO, USA) in fresh water and killed by decapitation. All experiments were approved by the Bioethics Committee at the University of Santiago de Compostela and the Consellería do Medio Rural e do Mar of the Xunta de Galicia (license Ref. JLPV/IId) and were performed in accordance with European Union and Spanish guidelines on animal care and experimentation.

Table 1 Animals used in each of the experiments

	Larvae	Young Adults	Mature adults
RNA extraction	8	-	-
***PmCCK* ISH**	6	5	3
PmCCK-8 + 5HT	3	3	3
PmCCK-8 + NPY	3	3	3
PmCCK-8 + TH	3	3	3
PmCCK-8+ GABA	4	2	-
PmCCK-8 + Glut	4	2	-
PmCCK-8 + SC Neurobiotin	4	-	-
Total:	31	10	6

In some cases, serial sections from the same animal (colour coded) were used for different experiments

Cloning and sequencing of the PmCCK precursor cDNA

Larvae were anesthetized by immersion in MS-222 (Sigma; see above) and the brain and spinal cord were dissected out under sterile conditions. Total RNA was isolated from these tissues using the TriPure reagent (Roche, Mannheim, Germany). The first-strand cDNA synthesis reaction from total RNA was catalysed with Superscript III reverse transcriptase (Invitrogen, Waltham, MA, USA) using random primers (hexamers; Invitrogen). For polymerase chain reaction (PCR) cloning, specific oligonucleotide primers (forward: 5′-TCTCTCTACCTGGGCTGGCT-3′; reverse: 5′-ATTCTTCATCCATAGCACTGCGTT-3′) were designed based on the *PmCCK* precursor cDNA sequence that was deposited in GenBank in 2009 by Dr. Y. Su (Jinling Institute of Technology) with accession number GQ421360.1. The amplified fragments were cloned into pGEM-T easy vectors (Promega, Madison, WI, USA) using standard protocols and sequenced by GATC Biotech (Cologne, Germany) using Sanger sequencing. To identify the gene encoding the *PmCCK* precursor, a BLAST search of the *P. marinus* genome (Smith et al. 2013) was conducted using the Ensembl database.

Alignment of the PmCCK precursor sequence with CCK precursor sequences from other chordates and phylogenetic analyses

The *PmCCK* cDNA sequence was translated to the corresponding amino acid sequence and analysed in the ExPASy website using SignalP 4.1 (Petersen et al. 2011) to predict putative signal peptides, PeptideCutter (Gasteiger et al. 2005) to predict potential cleavage sites, and The Sulfinator (Monigatti et al. 2002) to predict putative tyrosine sulfation sites. To further investigate the relationship of PmCCK with CCK-type precursors from other species, a phylogenetic analysis was performed using the neighbour-joining method. The amino acid sequence of PmCCK was aligned with precursors from other species using MUSCLE (ten iterations; substitution matrix BLOSUM62; see Supplementary Figure 1 for the alignment used for the tree and for the accession numbers of the sequences). The tree was constructed in MEGA 7. The percentage of replicate trees in which the associated taxa clustered together in the bootstrap test (5000 iterations) are shown next to the branches. The substitution model used was the Jones–Taylor–Thornton model. The tree is drawn to scale, with branch lengths in the same units as those of the evolutionary distances used to infer the phylogenetic tree. The C-terminal region of the precursor protein alignment was used to identify potential CCK-type peptides derived from PmCCK, as shown in Fig. 1. Conserved residues were highlighted using the software BOXSHADE (http://www.ch.embnet.org/software/BOX_form.html) with 70% conservation as the minimum for highlighting.

In situ hybridization

Templates for in vitro transcription were prepared by PCR amplification as follows. A 421-base pair (bp) fragment of the *PmCCK* precursor sequence was obtained using the primers mentioned above. In this case, the reverse primer included the sequence of the universal T7 promoter (TAA GCTTTAATACGACTCACTATAGGGAGA). For the generation of sense probes, the sequence of the T7 promoter was included in the forward primers. Digoxigenin (DIG)-labelled riboprobes were synthesized using the amplified fragments as templates and following standard protocols using a T7 polymerase (Nzytech, Lisbon, Portugal).

ISH experiments were performed as previously described for TH or 5-ht1a receptor riboprobes (Barreiro-Iglesias et al. 2010a; Cornide-Petronio et al. 2013). Briefly, the brains/rostral spinal cords of larvae and young and mature adults were dissected out and fixed by immersion for 12 h in 4% paraformaldehyde (PFA) in phosphate-buffered saline (PBS) at 4 °C. Then, they were cryoprotected with 30% sucrose in PBS, embedded in Tissue Tek (Sakura, Torrance, CA, USA), frozen in liquid nitrogen-cooled isopentane, and cut serially on a cryostat (14 µm thickness) in transverse planes. Sections were mounted on Superfrost® Plus glass slides (Menzel, Braunschweig, Germany). The sections were incubated with the *PmCCK* DIG-labelled antisense or sense riboprobes (1 µg/mL) at 70 °C overnight in hybridization mix and treated with RNAse A (Sigma) in the post-hybridization washes. Then, the sections were incubated with a sheep anti-DIG antibody conjugated to alkaline phosphatase (1:2000; Roche) overnight at 4 °C. Staining was conducted in BM Purple (Roche) at 37 °C until the signal was clearly visible. Finally, the sections were mounted in Mowiol® (Sigma). No staining was observed in the sections incubated with the sense probe.

Generation of a novel anti-PmCCK-8 antibody

A modified PmCCK-8 peptide (CDY(SO_3)IGWMDF-NH_2) with the addition of a cysteine residue to the N-terminus was synthesized by Biomedal (Sevilla, Spain) to enable coupling to KLH. A rabbit (8 weeks old, New Zealand White) was first immunized subcutaneously with the peptide-KLH conjugate (400 mg) emulsified in Freund's complete adjuvant. After 4 weeks, the rabbit was immunized once weekly for 2 weeks by intramuscular injection of the peptide–KLH conjugate (200 mg) emulsified in Freund's complete adjuvant. Pre-immune (negative control with no antibodies present) and post-immunization bleeds were collected. 2.5 mL of antiserum from the final bleed were purified using a protein A-Sepharose column (GE Healthcare, Little Chalfont, UK) and the purified antibodies were used for the immunohistochemical analyses.

Tissue processing for immunohistochemistry

For single or double immunohistochemistry, the heads or brains of larvae and brains of adults were fixed by immersion in 4% PFA in 0.05 M Tris-buffered saline pH 7.4 (TBS) for 4–12 h or in freshly prepared 5% glutaraldehyde and 1% sodium metabisulfite in TBS for 16 h at 4 °C. The samples were then rinsed in TBS (PFA fixed samples) or TBS with 1% sodium metabisulfite (glutaraldehyde fixed samples), cryoprotected with 30% sucrose in TBS, embedded in Tissue Tek (Sakura), frozen in liquid nitrogen-cooled isopentane, and cut serially on a cryostat (14 µm thickness) in transverse planes. Sections were mounted on Superfrost® Plus glass slides (Menzel). Some samples of gut from lamprey larvae were processed in parallel.

PmCCK-8 and TH, GABA, or glutamate double immunofluorescence experiments

Some samples fixed with 4% PFA were incubated with the purified rabbit polyclonal anti-PmCCK-8 antibody (dilution

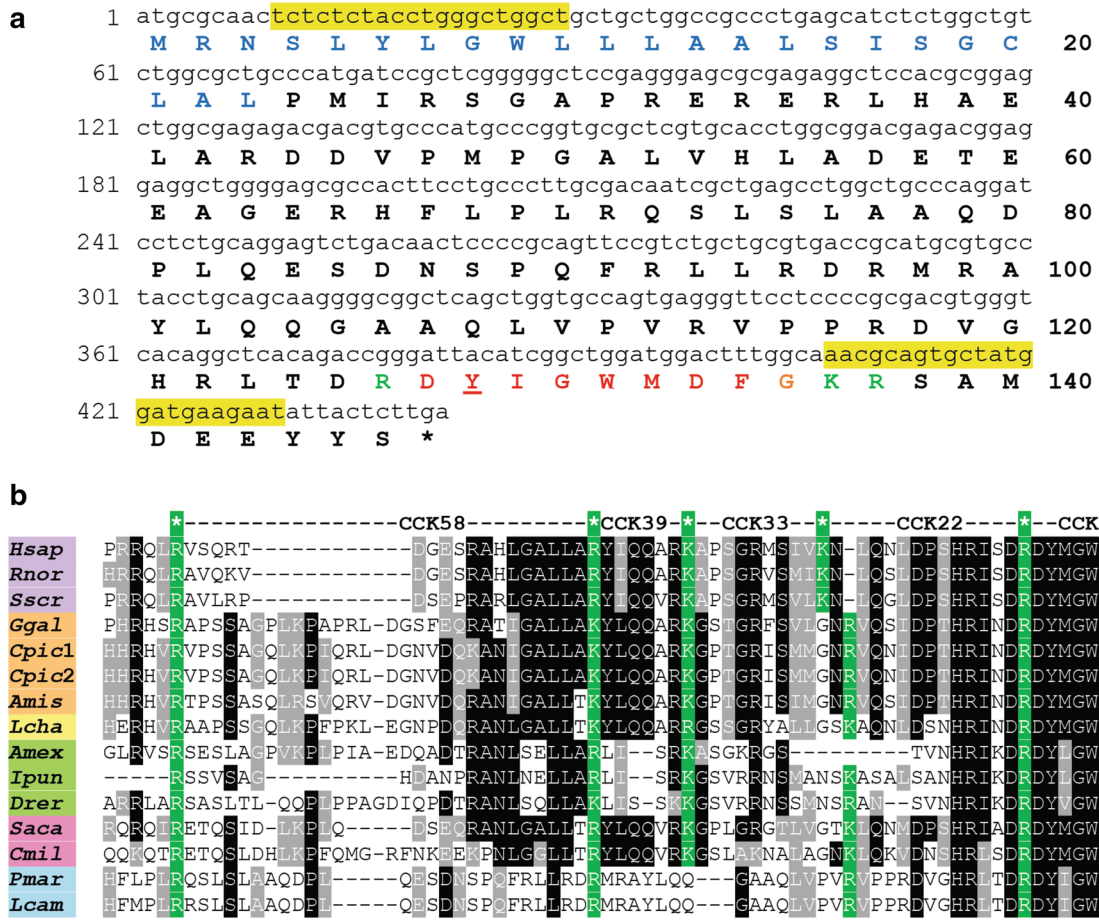
a
1 atgcgcaactctctctacctgggctggctgctgctggccgccctgagcatctctggctgt
M R N S L Y L G W L L L A A L S I S G C 20
61 ctggcgctgcccatgatccgctcgggggctccgagggagcgcgagaggctccacgcggag
L A L P M I R S G A P R E R E R L H A E 40
121 ctggcgagagacgacgtgcccatgcccggtgcgctcgtgcacctggcggacgagacggag
L A R D D V P M P G A L V H L A D E T E 60
181 gaggctggggagcgccacttcctgcccttgcgacaatcgctgagcctggctgcccaggat
E A G E R H F L P L R Q S L S L A A Q D 80
241 cctctgcaggagtctgacaactccccgcagttccgtctgctgcgtgaccgcatgcgtgcc
P L Q E S D N S P Q F R L L R D R M R A 100
301 tacctgcagcaaggggcggctcagctggtgccagtgagggttcctccccgcgacgtgggt
Y L Q Q G A A Q L V P V R V P P R D V G 120
361 cacaggctcacagaccgggattacatcggctggatggactttggcaaacgcagtgctatg
H R L T D R D Y I G W M D F G K R S A M 140
421 gatgaagaattattactcttga
D E E Y Y S *
b
CCK58
CCK39
CCK33
CCK22
CCK8
Hsap
Rnor
Sscr
Ggal
Cpic1
Cpic2
Amis
Lcha
Amex
Ipun
Drer
Saca
Cmil
Pmar
Lcam
c
Homo sapiens
Rattus norvegicus
Sus scrofa
Chrysemys picta bellii 1
Chrysemys picta bellii 2
Alligator mississippiensis
Gallus gallus
Latimeria chalumnae
Astyanax mexicanus
Danio rerio
Ictalurus punctatus
Squalus acanthias
Callorhinchus milii
Petromyzon marinus
Lethenteron camtschaticum
Ciona intestinalis
55
99
99
99
94
89
60
99
51
98
100
Legend
Mammalia
Sauropsida
Sarcopterygii
Actinopterygii
Chondrichthyes
Agnathans
Urochodata
0.2

◂**Fig. 1** Identification of a CCK-type precursor in the sea lamprey *P. marinus*. **a** Nucleotide and protein sequence of the PmCCK precursor. The signal peptide sequence is shown in blue and cleavage sites that give rise to the putative PmCCK-8 peptide are shown in green. The putative PmCCK-8 mature peptide is indicated in red, with the C-terminal glycine, which is substrate for amidation, shown in orange. The tyrosine residue that is predicted to be sulfated in mature peptide is underlined. The primers used for cloning of a fragment of the *PmCCK* precursor cDNA are highlighted in yellow. **b** Alignment of the C-terminal region of CCK-type precursor proteins from selected vertebrate species. Conserved residues are highlighted, with conservation in more than 80% of sequences shown in black and with conservative substitutions shown in grey. Conserved known or predicted cleavage sites are highlighted in green. The peptides corresponding to CCK-8, CCK-22, CCK-33, CCK-39, and CCK-58 are shown above the alignment. **c** Neighbour-joining tree showing relationships of CCK-type precursors in selected chordate species. The percentages of replicate trees in which the associated taxa clustered together in the bootstrap test (5000 replicates) are shown next to the branches. The analysis was conducted in MEGA 7. Species names in the alignment (**b**) are as follows: *Pmar* (*P. marinus;* highlighted with an arrow), *Lcam* (*Lethenteron camtschaticum*), *Hsap* (*Homo sapiens*), *Rnor* (*Rattus norvegicus*), *Sscr* (*Sus scrofa*), *Ggal* (*Gallus gallus*), *Cpic* (*Chrysemys picta belli*), *Amis* (*Alligator mississippiensis*), *Lcha* (*Latimeria chalumnae*), *Ipun* (*Ictalurus punctatus), Amex* (*Astyanax mexicanus*), *Drer* (*Danio rerio*), *Saca* (*Squalus acanthias*), and *Cmil* (*Callorhinchus milii*). In the alignment (**b**) and phylogeny (**c**), species names are highlighted in taxon-specific colours: blue (agnathans), purple (mammals), orange (sauropsids), yellow (lobe-finned fishes), green (ray-finned fishes), pink (cartilaginous fishes), and grey (urochordates). The accession numbers and the alignment of the sequences used to build this phylogenetic tree are shown in Supplementary Figure 1

1:200) at 4 °C for 72 h (Table 2). Other samples fixed in 4% PFA were processed for double immunofluorescence experiments using a cocktail of a mouse monoclonal anti-tyrosine hydroxylase (TH) antibody (dilution 1:1,000; Millipore, Temecula, C; Cat# MAB318; lot 0509010596; RRID: AB_2201528; immunogen: TH purified from PC12 cells) (Table 2) in combination with the anti-PmCCK-8 antibody. Samples fixed in 5% glutaraldehyde were processed for double immunofluorescence experiments using a cocktail of a mouse monoclonal anti-GABA antibody (dilution 1:1,200; Sigma; Cat# GB-69; RRID: AB_2314453; lot. 075K4795; immunogen: purified GABA conjugated to BSA) or a mouse monoclonal anti-glutamate (Glu) antibody (dilution 1:1,000; Swant, Bellinzona, Switzerland; Cat# mAB; RRID: AB_10013460; immunogen: purified L-Glu conjugated to BSA) (Table 2) in combination with the anti-PmCCK-8 antibody. Primary antibodies were diluted in TBS (PFA fixed samples) or TBS with 1% metabisulfite (glutaraldehyde fixed samples) containing 15% normal goat serum and 0.2% Triton as detergent.

For double detection of PmCCK-8 and TH, GABA, or Glu by indirect immunofluorescence, the sections were rinsed in TBS and incubated for 1 h at room temperature with a cocktail of Cy3-conjugated goat anti-rabbit (1:200; Millipore; Burlington, MA) and FITC-conjugated goat anti-mouse (1:100; Millipore) antibodies (Table 2). Sections were rinsed in TBS and distilled water and mounted with Mowiol (Sigma).

PmCCK-8 and 5-HT or neuropeptide Y double immunofluorescence using two primary rabbit polyclonal antibodies

For the simultaneous detection of PmCCK-8 and 5-HT, or PmCCK-8 and neuropeptide Y (NPY), we adapted a microwaving method for double indirect immunofluorescence with primary antibodies from the same species (Tornehave et al. 2000) as previously described (Barreiro-Iglesias et al. 2017). Some samples fixed with 4% PFA were incubated with the rabbit polyclonal anti-PmCCK-8 antibody (dilution 1:200) at room temperature overnight, rinsed in TBS, and incubated with the Cy3-conjugated goat anti-rabbit antibody (1:200) at room temperature for 1 h. After PmCCK-8 immunofluorescence, samples were submerged in 10 mM citrate buffer (pH 6.0) in plastic jars placed in a recipient with water and microwaved at 700 W for 5 min in a microwave oven (NVR 6124M, Nevir, Madrid, Spain). This treatment was repeated five times replacing the citrate buffer each time. After microwaving, the slides were left in the citrate buffer at room temperature for 20 min. Then, the sections were incubated with either a rabbit polyclonal anti-5-HT antibody (dilution 1:2,500; Immunostar, Still Water, MN, USA; code 20080; lot 431001; RRID: AB_572263; immunogen: 5-HT-formaldehyde-BSA conjugate) (Table 2) or a rabbit polyclonal anti-NPY antibody (dilution 1:600; Sigma, Cat# N9528; lot 057K4869; RRID: AB_260814; immunogen: synthetic porcine NPY conjugated to KLH) (Table 2) at room temperature overnight, rinsed in TBS and incubated for 1 h at room temperature with an Alexa Fluor 488-conjugated donkey anti-rabbit antibody (diluted 1:100; Thermo Fisher Scientific Inc., Waltham, MA) (Table 2). Slides were rinsed in TBS and distilled water and mounted with Mowiol (Sigma).

Antibody characterization

The antiserum and the purified fraction of anti-PmCCK-8 antibody were tested for specificity with an enzyme-linked immunosorbent assay (ELISA) using standard methods. The antiserum, the purified antibody (at concentrations from 1:1000 to 1:100,000) and the pre-immune serum (1:1000) were tested against the synthetic PmCCK-8 peptide without KLH (at a concentration of 1 mM) in the ELISA. Both the antiserum and the purified fraction gave a positive signal at all the tested concentrations, while the very low signal registered with the pre-immune serum was the same as the one obtained in the negative controls with PBS only. Moreover, immunostaining of sections was completely abolished

Table 2 Details on the antibodies used in this study

Antigen	Immunogen	Manufacturer, species in which the antibody was generated, Catalogue#, RRID	Dilution
PmCCK-8	CDY(SO3)IGWMDF-NH2 coupled to KLH	Biomedal, rabbit polyclonal (not commercially available)	1:200
Tyrosine hydroxylase	TH purified from PC12 cells	Millipore, mouse monoclonal, Cat# MAB318, RRID:AB_2201528	1:1000
GABA	Purified GABA conjugated to BSA	Sigma, mouse monoclonal, Cat# GB-69, RRID:AB_2314453	1:1200
Glutamate	Purified L-glutamate conjugated to BSA	Swant, mouse monoclonal, Cat# mAB 2D7, RRID:AB_10013460	1:1000
Serotonin	5-HT conjugated to BSA	Immunostar, rabbit polyclonal, Cat# 20080, RRID:AB_572263	1:2500
Neuropeptide Y	Synthetic porcine neuropeptide Y conjugated to KLH	Sigma, rabbit polyclonal, Cat# N9528, RRID:AB_260814	1:600
Rabbit immunoglobin	Rabbit immunoglobin	Millipore, goat, Cy3-conjugated, Cat#AP132C, RRID:AB_92489	1:200
Rabbit immunoglobin	Rabbit immunoglobin	Thermo Fisher, donkey, Alexa Fluor 488-conjugated, Cat# A21206, RRID:AB_2535792	1:100
Mouse immunoglobin	Mouse immunoglobin	Millipore, mouse, FITC-conjugated, Cat# AQ303F, RRID:AB_92818	1:100

The PmCCK-8 antibody can be provided by the corresponding author upon reasonable request

after pre-adsorption of the anti-PmCCK-8 antibody with the synthetic peptide without KLH (at a concentration of 20 µM overnight at 4 °C before the primary antibody incubation of the sections). In addition, the pattern of PmCCK-8-ir neuronal populations in the CNS matches the pattern of *PmCCK* transcript expressing populations seen by ISH (see "Results"), which further supports the specificity of the antibody.

The specificity of the anti-TH antibody was tested by the supplier. This antibody has been used in immunohistochemical studies of lamprey brain and retina (Pierre et al. 1997; Villar-Cerviño et al. 2006; Barreiro-Iglesias et al. 2010a, 2017). The anti-TH antibody was tested in western blots of sea lamprey and rat brain protein extracts in our laboratory, which revealed bands of similar size for the sea lamprey and rat TH enzymes (Barreiro-Iglesias et al. 2008b).

The monoclonal anti-GABA antibody has been evaluated for activity and specificity by the supplier, by dot-blot immunoassay. No cross-reaction was observed with BSA, L-alpha-aminobutyric acid, L-glutamic acid, L-aspartic acid, glycine, delta-aminovaleric acid, L-threonine, L-glutamine, taurine, putrescine, L-alanine or carnosine. The antibody showed weak cross-reaction with beta-alanine. Furthermore, the sections of the brain and retina of sea lamprey incubated with this antibody revealed the same pattern of immunostaining observed in studies with other anti-GABA antibodies (Villar-Cerviño et al. 2006; Robertson et al. 2007). In addition, the antibody has been tested in our laboratory in western blots of sea lamprey brain protein extracts (Villar-Cerviño et al. 2008). No protein band was stained in these blots. Moreover, pre-absorption of this GABA antibody with BSA did not block immunostaining in lamprey and immunostaining of sections was completely abolished after pre-absorption of the diluted anti-GABA antibody with a GABA-BSA conjugate (Barreiro-Iglesias et al. 2009a; Villar-Cerviño et al. 2009).

The mouse monoclonal anti-Glu antibody was raised against a glutaraldehyde-linked L-glutamate-BSA conjugate by Dr. P. Streit (Liu et al. 1989), and this clone was made commercially available through Swant. This antibody has been characterized with respect to cross-reactivity by antibody dilution experiments as well as by pre-absorption experiments (Adám and Csillag 2006) and it has been used in the previous studies of the sea lamprey brain and spinal cord (Fernández-López et al. 2012, 2016, 2017; Barreiro-Iglesias et al. 2017). The monoclonal anti-Glu antibody used in the present investigation showed the same pattern of glutamatergic neuronal populations in the adult sea lamprey brain as that previously described when using two different polyclonal anti-Glu antibodies. More importantly, all these anti-Glu antibodies reveal the same distribution of glutamatergic neuronal populations observed by vesicular glutamate transporter (VGlut) ISH (Villar-Cerviño et al. 2011, 2013).

The specificity of the anti-5-HT antibody was tested by the supplier, who reported no detectable cross-reactivity with tryptamine, 5-methoxytryptamine, L-tryptophan, 5-hydroxytryptophan, dopamine, norepinephrine, or adrenaline. The 5-HT antibody used was tested in western blots of sea lamprey brain extracts in our laboratory (Villar-Cerviño

et al. 2006). No protein band was detected in these blots. Moreover, immunostaining of sections was completely abolished after pre-adsorption of the anti-5-HT antibody with 5-HT-BSA conjugates (Abalo et al. 2007).

The anti-NPY antibody reacts with human NPY conjugated to BSA in dot blots. The antiserum shows no cross-reactivity in dot blots with substance P, neurokinin A, neurokinin B, vasoactive intestinal peptide, calcitonin gene-related peptide (rat), calcitonin, and somatostatin conjugated to BSA, or BSA. The anti-NPY antibody cross-reacts with porcine PYY-BSA conjugates in dot blots; however, cross-reactivity of porcine PYY with respect to porcine NPY (100%) was lower than 1%, as determined by radioimmunoassay (manufacturer's technical information). The mature lamprey NPY and PYY peptides display 83% (30 out of 36 positions) and 69% (25 out of 36) identity with mammalian NPY, respectively (Söderberg et al. 1994; Montpetit et al. 2005). Moreover, the staining pattern observed in the spinal cord with this antibody is similar to that reported by Brodin et al. (1988) with a different NPY antibody and clearly differed from that observed by these authors with a PYY antibody. We further tested the specificity of this antibody in lamprey by pre-absorption experiments with NPY, PYY, and PP (Barreiro-Iglesias et al. 2010b). Immunostaining of sections was completely abolished after pre-absorption of the diluted anti-NPY antibody with 10 µM porcine NPY (Sigma). However, the anti-NPY antibody immunostaining was not abolished after pre-absorption with 10 µM porcine PYY (Sigma) or 10 µM avian PP (Sigma), and the neuronal distribution of immunoreactivity in these pre-absorption experiments matched with that observed using non-absorbed anti-NPY antibody in parallel series of sections (Barreiro-Iglesias et al. 2010b).

As general controls for the secondary antibodies, sections were processed as above, except that the primary antiserum was omitted. No staining was observed in these controls.

Retrograde tract-tracing study of spinal cord-projecting PmCCK-8-ir neurons

The origin of PmCCK-8-ir fibres observed in the spinal cord was investigated by neuronal tract-tracing combined with immunofluorescence. Tract-tracing experiments were performed in larval samples to label descending neurons that innervate the spinal cord. Neurobiotin (NB, 322.8 Da molecular weight; Vector; Burlingame, CA, USA) was used as a tracer. The larval spinal cord was exposed by a longitudinal incision made in the dorsal region of the body at the level of the fifth gill and completely cut with Castroviejo scissors. The tracer was applied in the rostral stump of the spinal cord with the aid of a minute pin (#000). The animals were allowed to recover at 19.5 °C with appropriate aeration conditions for 7 days to allow transport of the tracer from the application point to the neuronal soma of descending neurons. Brains of these larvae were fixed with 4% PFA as above and processed for PmCCK-8 immunofluorescence. Then, the sections were incubated at room temperature with Avidin D-FITC conjugated (dilution 1:1,000; Vector; Cat#: A-2001) diluted in TBS containing 0.3% Triton X-100 for 4 h to reveal the presence of neurobiotin. Slides were rinsed in TBS and distilled water and mounted with Mowiol (Sigma).

Nuclear counterstain

Nuclear counterstain was carried out after immunofluorescence by immersing the slides in 0.5 µg/mL bisbenzimide (Sigma) in TBS for 10 s before mounting.

Image acquisition and montage

Confocal photomicrographs were taken with a TCS-SP2 spectral confocal laser microscope (Leica Microsystems, Wetzlar, Germany). Data were acquired by use of appropriate laser lines and narrow spectral windows tuned to the specific absorption and emission wavelengths of each fluorescent marker (bisbenzimide, FITC or Cy3). Confocal projections of stacks were done with the LAF suite (Leica) or with ImageJ (NIH free software). Fluorescence photomicrographs were obtained with an AX70 epifluorescence microscope equipped with a DP70 digital camera (Olympus, Tokyo, Japan). Plates of photomicrographs and minimal bright/contrast adjustments were composed with Photoshop CS (Adobe). For plate presentation, some red fluorescent photomicrographs were changed to grey scale, inverted and adjusted for brightness and contrast with Photoshop. Drawings were done with CorelDraw 12.

Results

Identification and cloning of the PmCCK precursor

A putative *PmCCK* cDNA sequence (441 bp) was deposited in GenBank in 2009 (accession number GQ421360.1). We used this sequence to perform a BLAST search of the sea lamprey genome (version 7.0) in the Ensembl database and found the same sequence in contig AEFG01025968 (scaffold GL476732: 308,169-310,751) encoded by two exons. Then, a fragment of the *PmCCK* cDNA (421 bp) was amplified by PCR, and cloned and sequenced, further confirming the sequence previously submitted to GenBank (Fig. 1a).

The corresponding amino acid sequence of PmCCK (146 amino acids; Fig. 1a) was analysed using the SignalP, Peptide Cutter, and Sulfinator tools, which revealed the presence of a 22 amino acid N-terminal signal peptide sequence, a dibasic

cleavage site in the C-terminal region and a tyrosine sulfation site in the putative PmCCK-8 mature peptide (Fig. 1a).

An alignment of the C-terminal region of PmCCK with CCK-type precursors from other vertebrates revealed many conserved sites. Importantly, there are several cleavage sites that are conserved in relation to the mammalian precursors. Cleavage of mammalian CCK-type precursors gives rise to peptides with different lengths, including CCK-58, CCK-33, CCK-22, and CCK-8 (Chandra and Liddle 2007). The alignment shows that many of the cleavage sites that produce these peptides in mammals can be found with different levels of conservation across the vertebrate species. The most conserved cleavage site is the one that gives rise to the CCK-8 peptide, which is found in mammals and all other vertebrate species. The putative PmCCK-8 mature peptide only has one amino acid substitution by comparison with CCK-8 peptides from most jawed vertebrates, including humans (I for M; Fig. 1b). The cleavage site that gives rise to the CCK-22 is present only in mammals. However, a basic residue (R) was found in a residue adjacent to where the cleavage site for CCK-22 is located in mammals, which may result in the generation of a CCK-21 peptide in the sea lamprey and in some other vertebrate species. The residue that gives rise to the CCK-33 is absent in the PmCCK precursor, but is conserved in other vertebrates. The residue that provides the cleavage site for CCK-39 is conserved across vertebrates, including lampreys. However, if cleavage occurs at this site in the lamprey the peptide generated would be shorter than CCK-39 (37 amino acids) due to the absence of some neighbouring residues. The residue that provides the cleavage site for the largest CCK-type peptide in mammals, CCK-58, is also conserved in the lamprey precursor and if used would generate a 63-residue peptide. The alignment also shows that a C-terminal FG motif, indicative of a C-terminal amidated phenylalanine in the mature peptides, is a conserved feature across all representative species (Fig. 1b). Based on an alignment of 16 selected CCK-type precursor protein sequences, a phylogenetic reconstruction was made using the neighbour-joining method and the tree was rooted using the sequence of the cionin precursor from the urochordate *C. intestinalis*. As shown in Fig. 1c, the PmCCK is grouped together with the CCK precursor from *Lethenteron camtschaticum* to form an agnathan clade (Fig. 1c). Furthermore, the position of the agnathan CCK-type precursor clade in the tree is consistent with the phylogenetic position of agnathans as the most basal extant vertebrates (Satoh et al. 2014; Delsuc et al. 2018).

Distribution of CCKergic cell populations in the lamprey brain

We studied the distribution of CCKergic cell populations in the brain of the sea lamprey using both ISH and immunofluorescence, employing specific *PmCCK* probes and antibodies against PmCCK-8. Immunofluorescence also revealed a number of labelled fibres distributed throughout most brain regions. Schematic drawings of transverse sections of brains of larvae and adults showing a composite view based on both ISH and immunofluorescence results are presented in Figs. 2 and 3. The terminology employed in this study for the various regions, nuclei, tracts, and identified neurons followed those used in other studies of our group (see Barreiro-Iglesias et al. 2017). Note that for descriptions of PmCCK populations in the hypothalamus, we use topographical names (dorsal, ventral) to facilitate comparison with most studies of this region in vertebrates, although according the prosomeric model (Pombal and Puelles 1999), these actually correspond to caudal and rostral regions, respectively, owing to the brain axis curvature at this region.

PmCCK transcript expression in the brain of larval sea lampreys

Analysis of the distribution of *PmCCK* mRNA-positive (*PmCCK*+) neurons was done by ISH in larvae of total body lengths between 80 and 110 mm. No *PmCCK*+ neurons were observed in the telencephalic hemispheres (Fig. 2a) and preoptic region of larvae. In the hypothalamus, a group of small *PmCCK*+ cells was observed in the nucleus of the postoptic commissure, which is located in the wall of the postoptic (anterior infundibular) recess (Figs. 2b, 4a). These *PmCCK*+ cells are located in outer cell rows of the thick mantle of periventricular cells. Some *PmCCK*+ cells are also present in the ventral hypothalamus and a few in the dorsal hypothalamus (Figs. 2c, 4b, c). In the alar diencephalon, a group of *PmCCK*+ cells is located in the prethalamus close to the ventral end of the thick cell rows of the thalamus (Fig. 4c, d). In the ventral part of the posterior tubercle, small *PmCCK*+ cells form a U-shaped arch below the ventricle. Larger *PmCCK*+ cells were found in the Schober's M5 nucleus of the mesencephalon (Schober 1964; Rodicio et al. 1995). Abundant small cells were also observed ventrally in the perioculomotor region (Figs. 2d, 4e, f) of the mesencephalon. In the hindbrain, *PmCCK*+ cells are present medially over and lateral to the medial longitudinal fasciculus (Figs. 2g, h, 4h, i) and more laterally near the sulcus limitans associated with the visceromotor column, extending between levels of the caudal trigeminal motor nucleus to the glossopharyngeal motor nucleus (Figs. 2g, 4g, h). These two populations form elongated columns with 1–4 cells in most sections on each side (about 80–110 cells in total for each population). Occasional *PmCCK*+ cells were also observed over the sulcus limitans. Unlike in adults (see below), no *PmCCK*+ cells were observed in the isthmus (Fig. 2e) or in the region of the nucleus of the solitary tract of the caudal hindbrain (Fig. 2h).

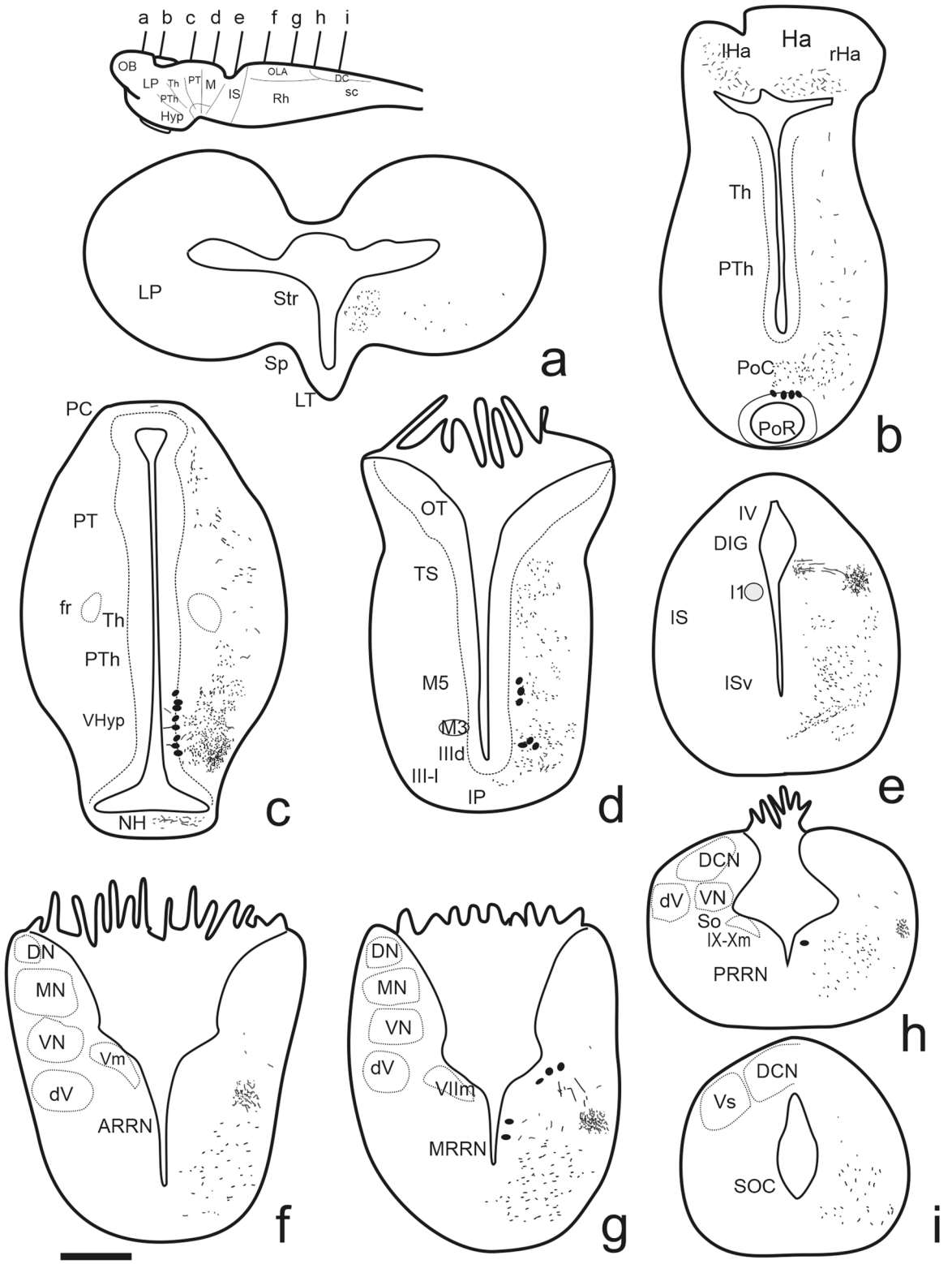

Fig. 2 Schematic drawings of transverse sections of the brain of a larval sea lamprey showing the composite distribution of *PmCCK* perikarya (black circles) and fibres (dots, dashes) based on ISH and immunofluorescence methods on the right, and the main brain structures on the left. The level of sections is schematically indicated in the upper left figurine. For abbreviations, see the list. Scale bar = 100 µm (applies to **a**–**i**)

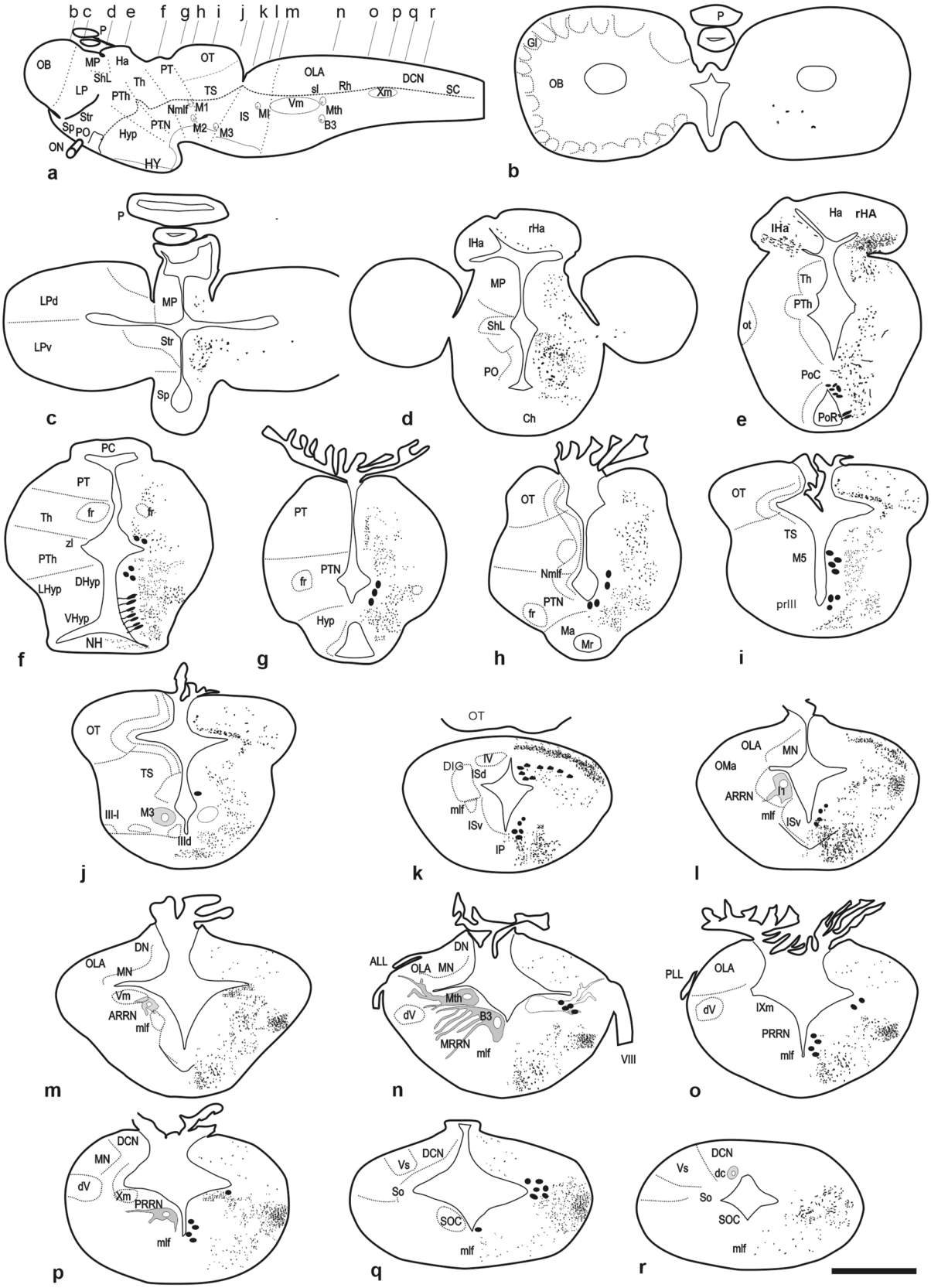
b c d e f g h i j k l m n o p q r
P
OB
MP
Ha
ShL
LP
Th
PT
OT
PTh
TS
OLA
sl
Rh
DCN
Xm
SC
Str
Nmlf
M1
IS
Vm
Mth
Sp
PO
PTN
M2
M3
B3
Hyp
ON
HY
a
Gl
b
LPd
LPv
c
rHa
lHa
d
Ch
Ha
rHA
e
ot
PoC
PoR
PC
fr
zl
DHyp
LHyp
VHyp
NH
f
g
Ma
Mr
h
TS
M5
prIII
i
III-l
IIId
j
DIC
IV
lSd
lSv
IP
k
OMa
MN
ARRN
l
m
ALL
MRRN
VIII
n
PLL
lXm
PRRN
o
dV
DCN
Vs
dc
So
SOC
mlf
p
q
r

◂**Fig. 3** Schematic drawings of transverse sections of the brain of an adult sea lamprey showing the composite distribution of *PmCCK* perikarya (black circles) and fibres (dots, dashes) based on ISH and immunofluorescence methods on the right, and the main brain structures on the left. The level of sections is schematically indicated in the upper left figurine. For abbreviations, see the list. Scale bar = 250 µm (applies to **b**–**r**)

PmCCK transcript expression in the brain of adult sea lampreys

We searched for possible changes in the *PmCCK*+ populations after metamorphosis and sexual maturation by analysing brains of young downstream pre-migratory adults (about 17 cm in length) and upstream migrating sexually mature sea lampreys (about 85 cm in length, about 2 years after transformation) (Figs. 3, 5, 6, 7, 8).

Young adults

In the brain of young adults, numerous *PmCCK*+ neurons were observed in the hypothalamus, diencephalon, mesencephalon, and rhombencephalon (Figs. 3, 5, 6, 7). Most populations correspond with those reported above in larvae, but new *PmCCK*+ populations were also observed in the rostral (isthmus) and caudal hindbrain.

The most rostral *PmCCK*+ populations were observed in the walls of the anterior infundibular (postoptic) recess. Two groups of *PmCCK*+ cells were distinguished (Figs. 3e, 5a, 7a). One of them forms an inverted U-shaped band over the recess, which corresponds with the nucleus of the postoptic commissure seen in larvae. Caudally to the postoptic commissure, this group appears in continuity with a bilateral band extending in the dorsal hypothalamus (Figs. 3f, 5b, 7b). These cells occupy a peripheral region of the thick periventricular band of cells. Other *PmCCK*+ cells are located more ventrally in the periventricular region, mostly in the inner cell rows of the periventricular region of the ventral hypothalamus (Figs. 3e, f, 5a, 7a).

In the prethalamus (alar prosomere 3; p3; see Pombal and Puelles 1999), a small and scattered group of *PmCCK*+ cells was observed in outer rows of the thickened band of cells of this region, clearly separated from the hypothalamic positive populations (Figs. 3f, 5d, 7c). A U-shaped band of *PmCCK*+ cells is also found at the level of the nucleus of the posterior tubercle (Figs. 3g, h, 5e, 7d). More caudally, a group of intensely stained *PmCCK*+ cells was observed in the basal region of prosomere 1 (p1) dorsally to the giant M2 cell (nucleus of the medial longitudinal fasciculus; Figs. 3h, 7e). In the midbrain dorsal tegmentum, a large group of *PmCCK*+ cells was observed in the Schober's M5 nucleus (Schober 1964) (Fig. 3i, j, 5g–i, 7f). A population of smaller *PmCCK*+ cells was also found in the perioculomotor ventral tegmentum till the level of the oculomotor nucleus (dorsomedial subnucleus) (Figs. 3i, 5h–i, 7g).

The *PmCCK*+ cell populations of the hindbrain are separated from those of the midbrain by a region without *PmCCK*+ cells. Unlike in larvae, the rostral isthmus shows a large group of intensely stained *PmCCK*+ cells located in the dorsal periventricular region (Figs. 3k, 6a, 7h). From this periventricular nucleus, intermediate and lateral populations of *PmCCK*+ cells extend laterally in direction to the entrance of the trigeminal nerve. All together, these populations are part of the dorsal isthmic grey (Fig. 7h). The periventricular *PmCCK*+ population is not observed at levels caudal to the giant I1 Müller cell. The scattered *PmCCK*+ cells of the intermediate and lateral populations are larger and have a smaller rostrocaudal extension than the periventricular population. In the caudal isthmic tegmentum, a fairly numerous *PmCCK*+ population is present in the small-celled region ventral to large reticular cells and over the interpeduncular nucleus, extending caudally till rostral trigeminal levels (i.e., the region showing the rostral trigeminal motoneurons) (Figs. 3k, l, 6b, c, 7i).

More caudally in the hindbrain, a long reticular population of small *PmCCK*+ reticular cells is located over and medial to the giant axons of the medial longitudinal fasciculus (note that along the hindbrain these fibres are much thinner than in the spinal cord) (Figs. 3o–q, 6f–h, 7k). These *PmCCK*+ cells are found both in clusters and intermingled among much larger reticulospinal neurons that are *PmCCK*-negative. These *PmCCK*+ cells are not observed at the level of the obex. In a young adult, we counted about 165 positive cells in this reticular population. A few *PmCCK*+ reticular neurons are found at intermediate levels between the vagal motor nucleus and the large (*PmCCK*-negative) medial reticular neurons (Fig. 6e). Other *PmCCK*+ cells are associated with the different parts of the visceromotor column (Figs. 3n–p, 6g, h, 7j, k). Scattered *PmCCK*+ cells are associated with the lateral part of the trigeminal motor nucleus (lateral reticular region) and the rostral level of the facial motor nucleus. More caudally, some *PmCCK*+ cells are observed close to the glossopharyngeal and vagal motor nuclei. In the caudal hindbrain, at levels close to the obex, a group of intensely *PmCCK*+ cells is present in the periventricular cell mantle just ventral to the dorsal column nucleus/descending trigeminal nucleus (Figs. 3q, 6h, i, 7l). We considered that these caudal neurons pertain to the nucleus of the solitary tract (see "Discussion").

Sexually mature upstream-migrating sea lamprey

The general distribution of *PmCCK*+ cells in mature adult lampreys is similar to that of young adults, although some changes in the appearance of populations were noted (Fig. 8). As observed in young adults, the most rostral

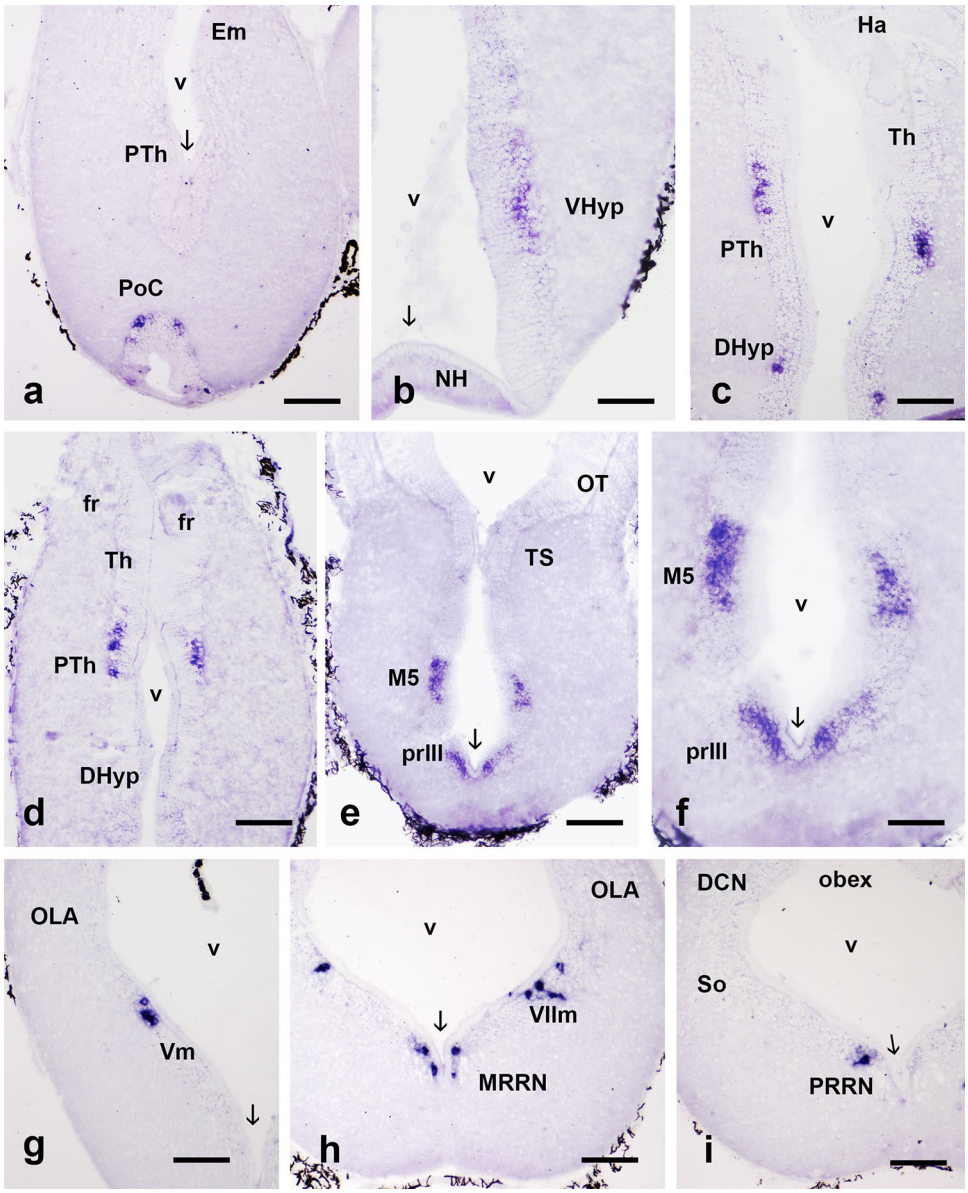

Fig. 4 Rostrocaudal transverse sections through the brain of a larval sea lamprey showing the distribution of *PmCCK*-positive neuronal populations. **a** Section at the level of the postoptic commissure. **b** Detail of the ventral hypothalamus adjacent to the neurohypophysis. **c**, **d** Sections showing *PmCCK* populations in the prethalamus and dorsal hypothalamus. **e**, **f** Section showing mesencephalic *PmCCK* populations. **g**–**i** Sections showing hindbrain *PmCCK* populations associated with motor nuclei and in rhombencephalic reticular regions. **f** is a detail of **e**. For abbreviations, see the list. The arrow in **a** points to the midline. Arrows in **b** and **e**–**i** point to the ventral midline. Dorsal is to the top. Note numerous melanophores (black cells) in the meninges. Scale bars = 200 µm (**a**, **c**, **e**, **g**, **h**, **i**), 100 µm (**b**, **c**, **f**)

PmCCK+ cells were observed in the walls of the postoptic recess (Fig. 8a, b). The *PmCCK*+ cells of the nucleus of the postoptic commissure showed faint-to-moderate signal and occupied outer periventricular regions (Fig. 8a–c). This population extends caudally in the dorsal hypothalamus (Fig. 8d). Instead, the ventral hypothalamic *PmCCK*+ cells were intensely stained, and most were found in the inner cell rows of the periventricular region of the ventral hypothalamus (Fig. 8a–c). The number of cells in these nuclei increased with respect that of young adults.

The *PmCCK*+ cells of the prethalamic group were scattered through a wider region than in young adults (Fig. 8d). From the nucleus of the posterior tubercle, a U-shaped band of *PmCCK*+ cells extends caudally till the perioculomotor region (Fig. 8e, f). A scarce group of intensely stained *PmCCK*+ cells is present in the basal region of p1 dorsally to the M2 cell (Fig. 3h). In the midbrain, the group of *PmCCK*+ cells located below the torus semicircularis (M5 nucleus of Schober 1964) shows intense staining (Fig. 8f).

In the dorsal isthmic grey, the periventricular group shows faintly stained small *PmCCK*+ cells and small groups of migrated *PmCCK*+ cells extend laterally (not shown). In the caudal isthmic tegmentum and the rostral region of the trigeminal motor nucleus, abundant *PmCCK*+ cells are intensely stained in the small-celled ventral reticular population of this region (Fig. 8g). At levels of the glossopharyngeal nerve entrance and motor nucleus, intensely stained *PmCCK*+ reticular neurons are observed in the medial region of the posterior reticular formation over the medial longitudinal fasciculus giant

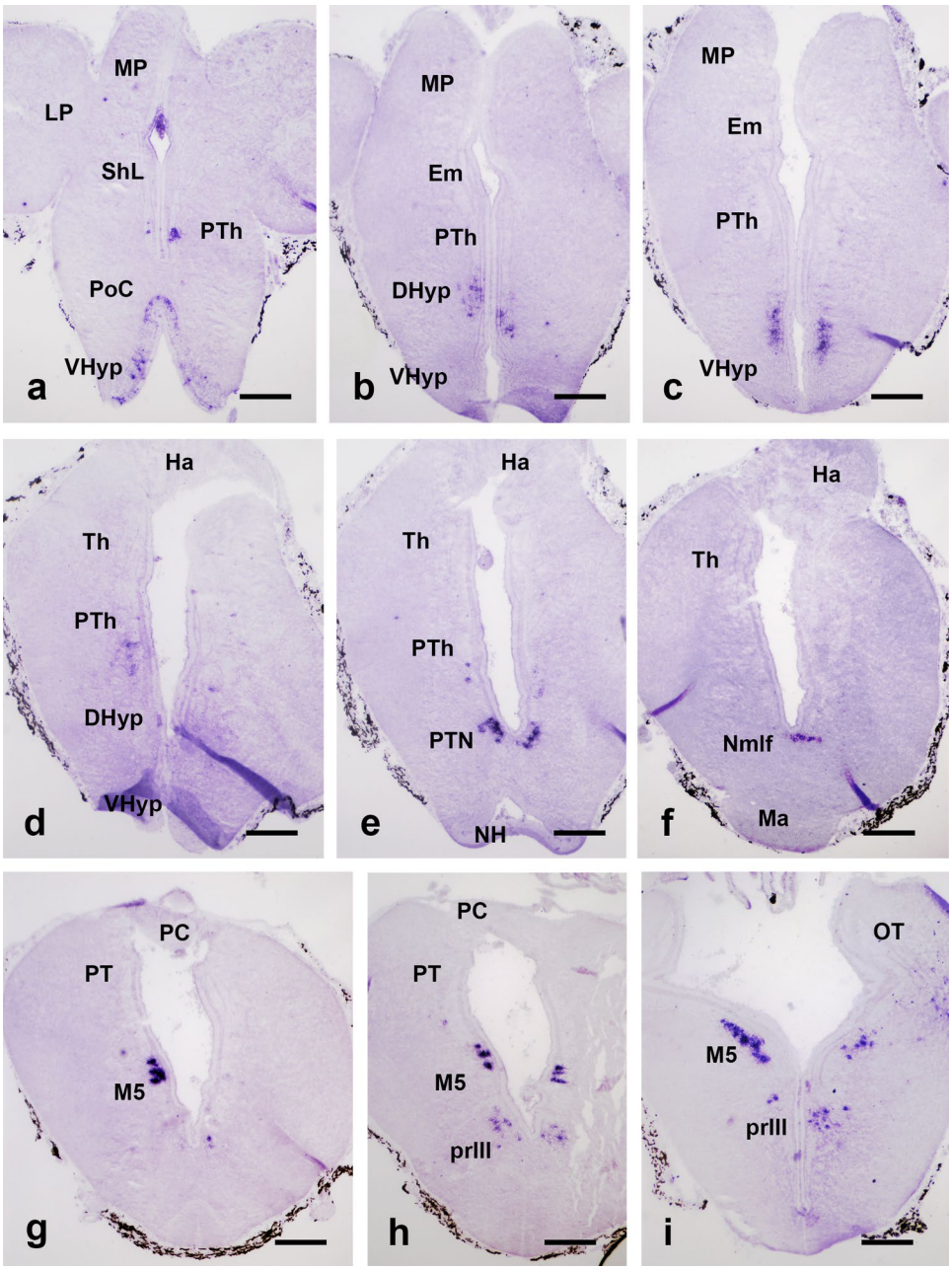

Fig. 5 Panoramic views of transverse sections through the prosencephalon and mesencephalon of a young adult lamprey in rostrocaudal sequence showing the location of *PmCCK*-positive neuronal populations in the hypothalamus (**a**–**c**), prethalamus (**d**), nucleus of the posterior tubercle (**e**), nucleus of the medial longitudinal fasciculus (**f**), and mesencephalic tegmentum (**g**–**i**). For abbreviations, see the list. Dorsal is to the top. Note numerous melanophores (black cells) in the meninges. Scale bars = 250 µm

axons (Fig. 8i). In the lateral reticular formation, scattered small *PmCCK* + reticular cells are associated with the caudal portion of the trigeminal motor nucleus (Fig. 8h) till rostral levels of the facial motor nucleus. More caudally, some *PmCCK* + cells are observed laterally close to the glossopharyngeal motor nucleus. At levels of the vagal motor nucleus, intermediate *PmCCK* + reticular neurons are present medially to the visceromotor column. In the caudal hindbrain, at levels close to the obex, intensely stained *PmCCK* + cells of the nucleus of the solitary tract noted in young adults extend in the periventricular cell mantle below the dorsal column nucleus/descending trigeminal nucleus (Fig. 8j).

Localization of PmCCK-8 immunoreactivity in the sea lamprey CNS

Immunohistochemistry with antibodies raised against the PmCCK-8 peptide revealed perikarya and a number of immunoreactive processes distributed throughout most brain regions (Figs. 2, 3). In general, the distribution of PmCCK-8-ir perikarya in larval and adult lampreys was similar to that reported above with *PmCCK* ISH in the same stages. In addition, immunohistochemistry revealed a rich innervation of most brain regions by PmCCK-8-ir processes, as schematically indicated in larval and adult brains (Figs. 2, 3). Although in most brain regions, fibres

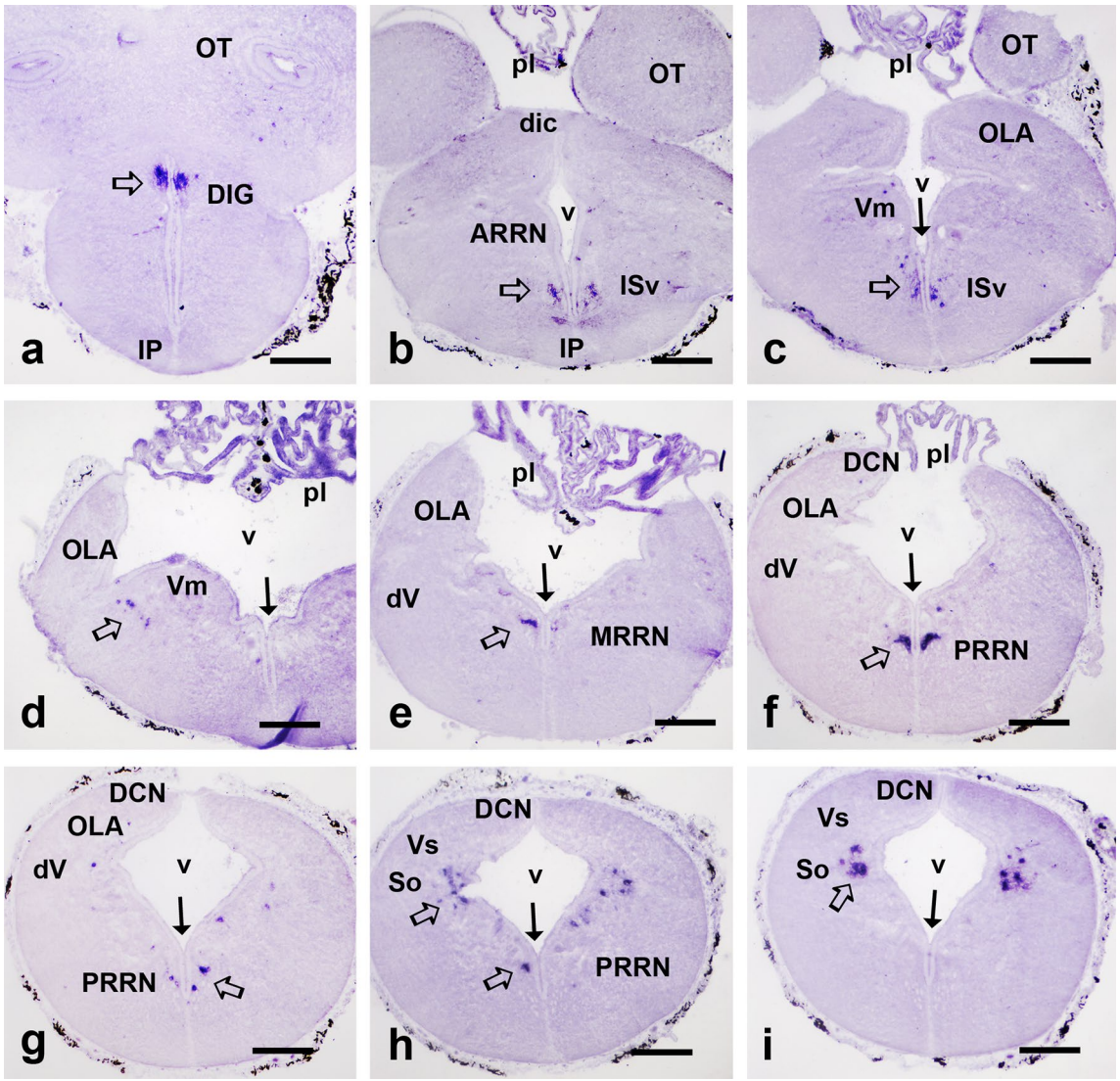

Fig. 6 Panoramic views of rostrocaudal transverse sections through the caudal optic tectum and rhombencephalon of a young adult lamprey showing the distribution of *PmCCK*-positive neuronal populations (outlined arrows). **a** Section showing positive cells in the periventricular region of the dorsal isthmic grey. **b**, **c** Sections showing ventral isthmic populations. **d** Section showing cells just lateral to the trigeminal motor nucleus. **e**, **f** Sections showing positive reticular cells close to the medial longitudinal fasciculus. **h**, **i** Sections showing a conspicuous population in the putative nucleus of the solitary tract. Thin arrows in **c**–**i** point to the ventral midline. For abbreviations, see the list. Dorsal is to the top. Note numerous melanophores (black cells) in the meninges. Scale bars = 250 µm

were scattered in neuropil areas, a conspicuous PmCCK-8-ir tract was observed in the hindbrain of larvae and adults. The pattern of PmCCK-8-ir innervation will be described in some detail in only a few brain regions (striatum, habenula, optic tectum, and isthmus). It should also be noted that in adults, the cell nuclei of large PmCCK-negative neurons showed weak autofluorescence signal but not their cytoplasm or processes. This autofluorescent signal was easily distinguishable from that of true PmCCK-8-ir cells, which show an intensely immunopositive fine granular material in their cytoplasm.

PmCCK-8-ir neurons in larval sea lamprey

In larval brains, PmCCK-8-ir neurons were observed in the hypothalamus, nucleus of the medial longitudinal fasciculus, midbrain tegmentum, and in hindbrain medial and lateral reticular populations (Figs. 2, 9, 10). In the hypothalamus, some small PmCCK-8-ir neurons were observed in the outer rows of the periventricular cell layer of the ventral hypothalamus (Figs. 2c, 9a, f, 10b, d). Some of these PmCCK-8-ir cells show long and thin apical dendrites ending in a small intraventricular club, i.e., they are cerebrospinal

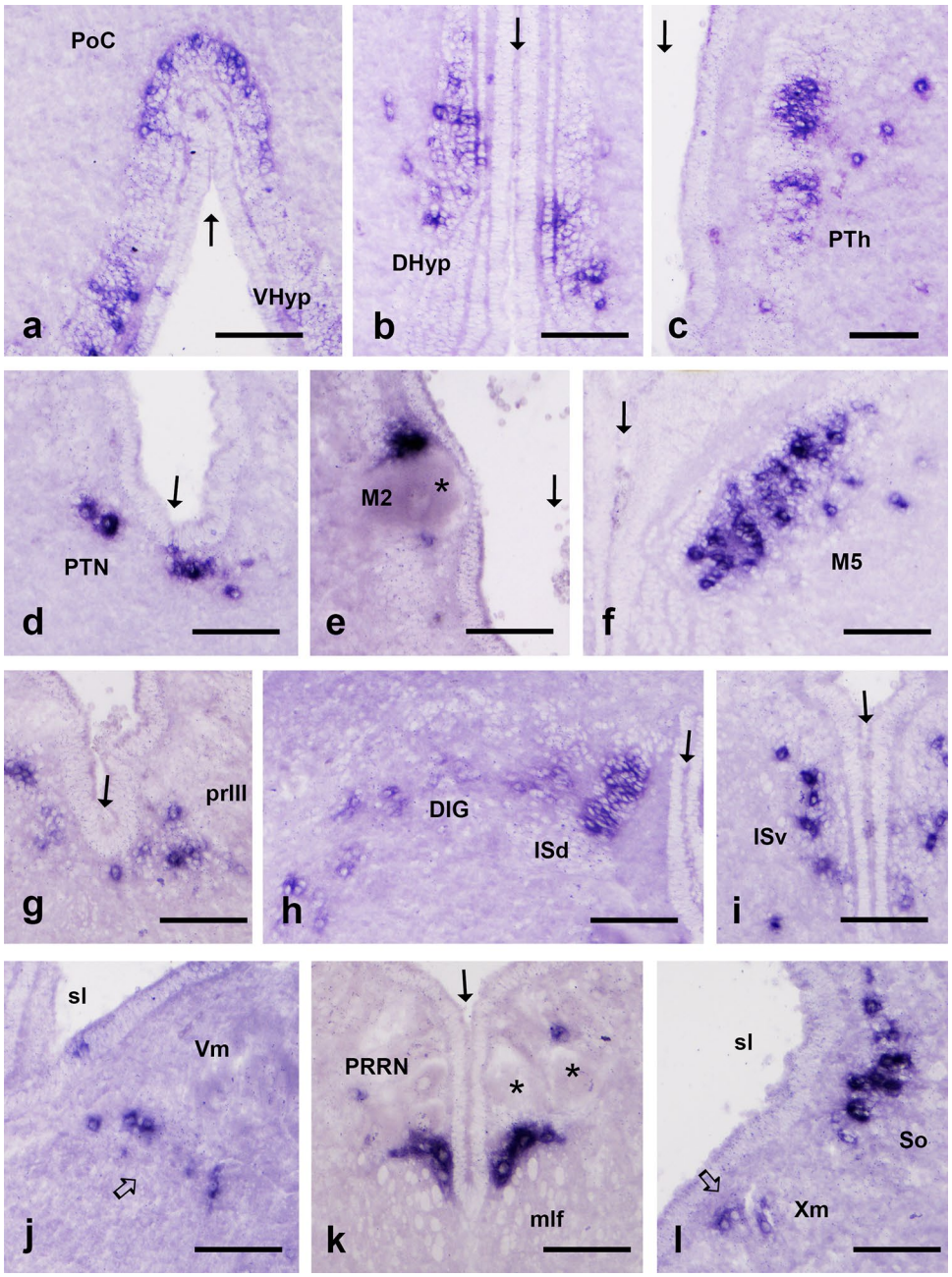

Fig. 7 Details of rostrocaudal transverse sections showing the *PmCCK*-positive neuronal populations of a young adult lamprey. **a**, **b** Nucleus of the postoptic commissure and ventral hypothalamus. **c** Prethalamus. **d** Posterior tubercle nucleus. **e** Nucleus of the medial longitudinal fasciculus with the M1 cell. **f** Midbrain M5 nucleus. **g** Perioculomotor region. **h** Dorsal isthmic grey showing small periventricular cells and the band of larger cells extending laterally as a wing. **i** Ventral isthmus population. **j** Cells lateral to the trigeminal motor nucleus. **k** Small reticular cells over the medial longitudinal fasciculus. **l** Neurons in the putative nucleus of the solitary tract and near the vagal motor nucleus. Asterisks in **e** and **k** indicate large reticulospinal neurons. Outlined arrows indicate small positive cells just lateral to the caudal trigeminal motoneurons (**j**) and cells medial to the vagal motoneurons (**l**). Thin arrows point to the midline. For abbreviations, see the list. Dorsal is to the top. Scale bars = 100 µm

fluid-contacting (CSF-c) cells. In the neuropil lateral to these bipolar cells, there are numerous PmCCK-8-ir beaded processes. In addition to ventral hypothalamic neurons, a few PmCCK-8-ir cells were observed in the dorsal hypothalamus (Fig. 10a). In the posterior tubercle and region of the nucleus of the medial longitudinal fasciculus, numerous small PmCCK-8-ir neurons were observed in the periventricular region of the ventricle floor (Fig. 9b, 14e). Caudally, PmCCK-8-ir cells were also observed in the M5 nucleus and perioculomotor region in the midbrain (Fig. 2d, 9g, 14d).

In the hindbrain of larvae, some PmCCK-8-ir neurons are associated with the lateral region of the facial motor nucleus and the caudal portion of the trigeminal motor nucleus (Figs. 2g, 9h, 14b). These PmCCK-8-ir cells are clearly larger than those of the midbrain and show a few dendrites and axons coursing ventrolaterally. In the reticular region of the hindbrain, a few spindle-shaped or triangular small PmCCK-8-ir neurons are associated with the medial longitudinal fasciculus near the midline (Figs. 2h, 9e, i, 14a).

PmCCK-8-ir neurons in adult sea lamprey

The PmCCK-8-ir neuronal populations observed in young adults and upstream migrated adults are roughly similar.

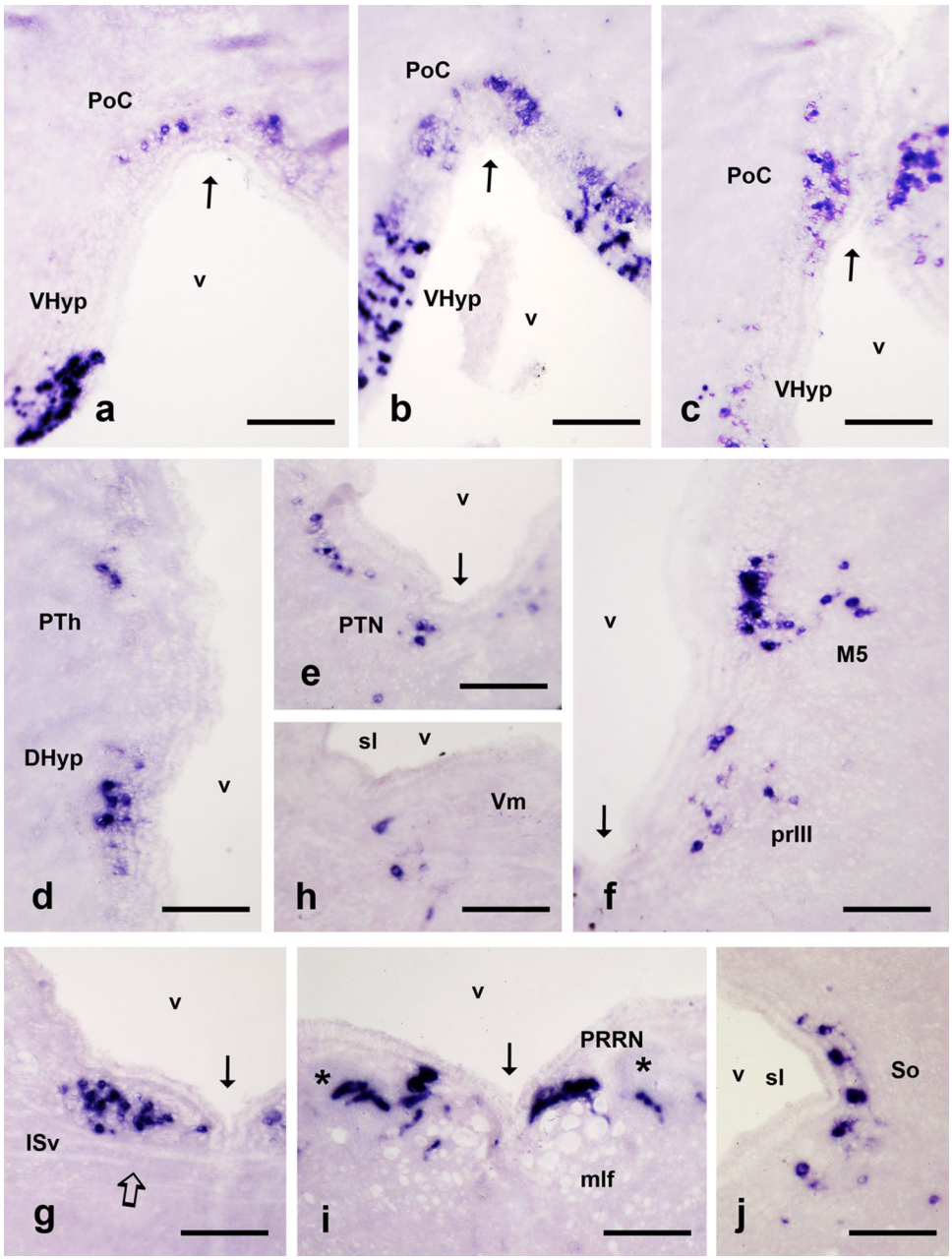

Fig. 8 Details of transverse sections showing the *PmCCK*-positive neuronal populations of an upstream-migrating adult lamprey. **a**–**c** Nucleus of the postoptic commissure and ventral hypothalamic populations. **d** Cells in prethalamus and dorsal hypothalamus. **e** Posterior tubercle populations. **f** Midbrain M5 and perioculomotor populations. **h** Ventral isthmic population. **i** Rhombencephalic reticular neurons over the mlf. **j** Positive population in the putative nucleus of the solitary tract. Asterisks in **i** indicate large reticulospinal neurons. Thin arrows (**a**–**c**, **e**, **f**, **g**, **i**) point to the midline. In **d** and **h,** the midline is to the right; in **j,** the midline is to the left. Outlined arrow in **g** points to thick commissural fibres coursing in the caudal isthmus below the *PmCCK* ventral population. For abbreviations, see the list. Dorsal is to the top. Scale bars = 200 µm

Accordingly, they will be described together but highlighting the main differences observed between them (Figs. 3, 11). In general, the locations of the PmCCK-8-ir populations coincide with those expressing the *PmCCK* precursor transcript, but some cells lack or exhibit only faint PmCCK-8 immunoreactivity. As noted with the expression of the *PmCCK* precursor, some PmCCK-8-ir populations of adults were not observed in larvae.

In young adults, the preoptic nucleus shows numerous small PmCCK-like-ir cells dorsal and lateral to the optic recesses, which do not correspond with any *PmCCK* + population described in adults or larval lampreys (see above). These cells mainly form a compact band separated from the ependymal layer by a fibrous layer, with a few neurons displaced at periependymal location (not shown). The perikarya of this region were PmCCK-8-negative in mature adults. In the hypothalamus of adults, a large dorsal population of small PmCCK-8-ir cells is distributed in the outer rows of periventricular cells (Fig. 3f). Ventrally, the PmCCK-8-ir cells are located in the inner periventricular row or among ependymocytes and show plump perikarya with a short conical ventricular dendrite (Figs. 3f, 11a). These ventral cells are larger than dorsal ones, and this ventral–dorsal difference is more conspicuous in mature migrating adults.

In the region of the nucleus of the posterior tubercle, scarce and small PmCCK-8-ir cells are observed below

the ventricle in the midline (Fig. 3g, h). At the level of the nucleus of the medial longitudinal fasciculus, some PmCCK-8-ir cells are also present in the lateral wall (Fig. 3h). These lateral cells are rather large and conspicuous in mature adults (Fig. 11b). More caudally, a group of intense PmCCK-8-ir cells with long lateral processes is observed in the cell rows of the Schober's M5 nucleus separated from the ventricle by a thick periventricular fibrous layer (Fig. 3i, j). Ventrally, some PmCCK-8-ir neurons are observed in the perioculomotor region near the giant M3 cell (Figs. 3i, 11c). These cells are conspicuous in mature adults.

Major differences between PmCCK-8-ir populations of larvae and adults are noted in the rostral hindbrain. In the isthmus of young adults, abundant PmCCK-8-ir periventricular cells are observed in dorsal regions over large isthmic reticular cells, and some migrated PmCCK-8-ir cells extend in a lateroventral band (dorsal isthmic grey), as noted with *PmCCK* ISH in adults (Figs. 3k, 11d–f, 12b). In the caudal isthmic–rostral trigeminal region, groups of small PmCCK-8-ir cells are found in the tegmental ventral reticular region (Figs. 3k, 12d). More caudally, some PmCCK-8-ir cells are scattered lateral to the facial motor nucleus (Figs. 3n, 11g). Bipolar or tripolar PmCCK-8-ir cells are observed in a thick cell band below the dorsal column/trigeminal descending nucleus that are separated from the ependymal layer by a thick fibre/neuropil layer. This cell population corresponds to the location of the putative nucleus of the solitary tract (Figs. 3q, 11h). In the caudal hindbrain of adults, some reticular PmCCK-8-ir cells are also located over the medial longitudinal fasciculus near the midline (Figs. 3q, 11i, 12c).

Brain innervation by PmCCK-8-ir fibres

The brain of the sea lamprey shows abundant PmCCK-8-ir fibres innervating many brain regions in both larvae and adults (Figs. 2, 3, 9, 10, 11, 12, 13, 14). The distribution of PmCCK-8-ir fibres in the adult brain is represented schematically in the Fig. 3, and examples of PmCCK-8-ir innervation of selected regions containing PmCCK-8-ir neurons are appreciable in Figs. 11 and 13. Most abundant PmCCK-8-ir fibres were observed in the hypothalamus and tegmental regions.

In larval lamprey brains, the telencephalic hemispheres are scarcely innervated by PmCCK-8-ir fibres excepting the striatum (Fig. 2a). PmCCK-8-ir fibres are abundant in the preoptic region and the hypothalamus (Fig. 10d, e). In the neurohypophysis, thin PmCCK-8-ir fibres are observed in inner zones (Fig. 10b). The posterior tubercle and region of the nucleus of the medial longitudinal fasciculus are innervated by fairly abundant PmCCK-8-ir fibres (Fig. 14e). In the right habenula, dense innervation by PmCCK-8-ir fibres is found in the ventral region but not in the dorsal region, and numerous PmCCK-8-ir fibres also innervate the left habenula (Fig. 2b), an innervation pattern that is similar to that reported using alpha-transducin (Gαt-S) immunoreactivity (Barreiro-Iglesias et al. 2017). In the midbrain, PmCCK-8-ir fibres are mainly located in the tegmental region (Figs. 2d, 14d), but are mostly lacking in the optic tectum, which is poorly developed in larvae (Fig. 2d). In the hindbrain, a conspicuous longitudinal tract of PmCCK-8-ir fibres courses in the ventrolateral region below the descending trigeminal root and extends rostrally to the dorsal isthmic region, where fibres of this tract bend medially and end on a small population of PmCCK-8-negative glutamatergic neurons in the periventricular region over the giant isthmic reticular cells (Figs. 2e–h, 9c, d, 14c). These fibres appear to arise from the PmCCK-8-ir cells accompanying the visceral column at facial-glossopharyngeal levels. Fibres of this PmCCK-8-ir tract also course caudally through the hindbrain. In addition, scattered PmCCK-8-ir fibres are distributed throughout the hindbrain reticular area, but they are scant or lacking in the octavolateralis region and in the nucleus of the dorsal column/descending trigeminal tract (Figs. 2f–i, 14b).

In the telencephalon of adult lampreys, the striatum receives rich PmCCK-8-ir innervation (Figs. 3c, d, 13b), but fibres are scarce in the lateral and medial pallium (Figs. 3b, c, 13a, b) and almost lacking in the olfactory bulb (Fig. 3a). A large number of PmCCK-8-ir fibres are observed in the preoptic region (which belongs to the subpallium) and the hypothalamus (Figs. 3d–h, 13c). In both young and mature adults, a compact tract of PmCCK-8-ir fibres decussates in the region of the postoptic commissure and can be followed towards the prethalamus and thalamus (not shown). In the habenula, conspicuous PmCCK-8-ir innervation is found in the same regions of larvae (ventral right habenula and left habenula), but these fibres are not present in dorsal habenular regions (Figs. 3d, e, 13d, e). In the dorsal midbrain, fairly abundant PmCCK-8-ir fibres are observed in deep tectal layers (Figs. 3i, j, 13f), which is unlike the larval tectum. Fairly abundant fibres are observed in midbrain tegmental regions (Figs. 3i, j, 13g).

At rostral rhombencephalic levels, a thick band comprised of numerous PmCCK-8-ir fibres courses from the region of the entrance of the trigeminal nerve towards the dorsomedial isthmus over the dorsal isthmic grey, crossing the midline in a dorsal isthmic commissure (over the decussation of the trochlear nerve), whereas only scarce fibres course toward the PmCCK-8-ir periventricular cell population (Figs. 3k, 11d). In mature adults, both the PmCCK-8-ir lateral tract and the dorsal isthmic commissure are very conspicuous. The tract can be followed along the hindbrain on a ventrolateral region below the trigeminal descending tract, disappearing at the transition with the spinal cord (Fig. 3l–q). Moreover,

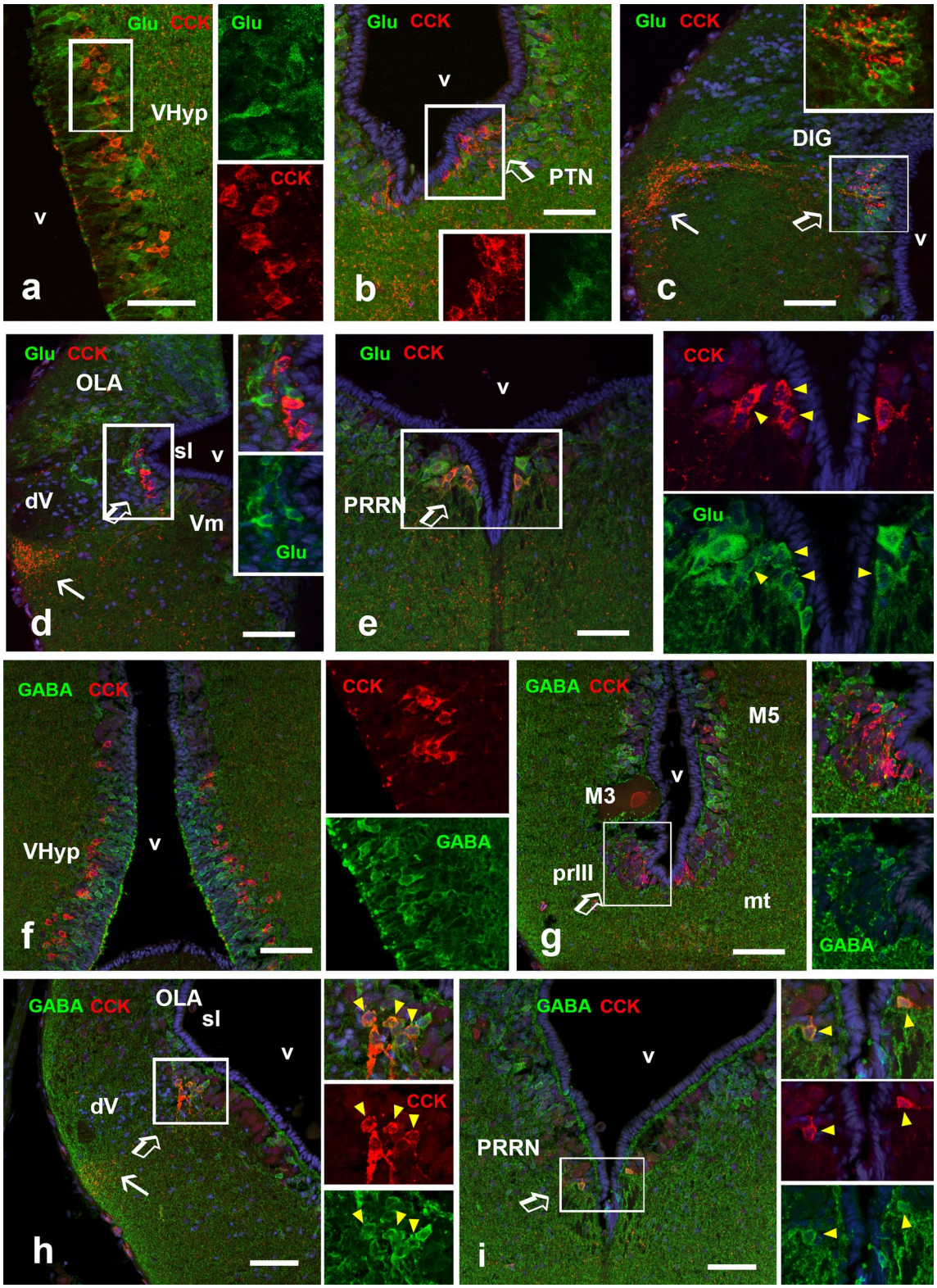
Glu CCK
Glu
CCK
VHyp
v
a
Glu CCK
v
PTN
b
Glu CCK
DIG
v
c
Glu CCK
OLA
sl
v
dV
Vm
Glu
d
Glu CCK
v
PRRN
e
CCK
Glu
GABA CCK
VHyp
v
f
CCK
GABA
GABA CCK
M5
v
M3
prIII
mt
g
GABA
GABA CCK
OLA
sl
v
dV
CCK
h
GABA CCK
v
PRRN
i

◂**Fig. 9** Confocal photomicrographs of double immunostained sections of larval brains showing PmCCK-8-ir (CCK, red channel) neuronal populations and co-distribution or co-localization with Glu or GABA immunoreactivities (green channel). **a** Photomicrograph and single channel details (squared area) showing PmCCK-8-ir CSF-c neurons co-distributed with glutamatergic cells in the ventral hypothalamus. **b** Photomicrograph and single-channel details (squared area) of the posterior tubercle showing co-distribution with Glu in the ventral small-celled PmCCK-8-ir population (outlined arrow). **c** Section of the isthmus showing the conspicuous ascending PmCCK-8-ir tract (thin arrow) projecting specifically on a glutamatergic periventricular population (outlined arrow). Inset is a two-channel detail of the squared area. **d** Photomicrograph of the PmCCK-8-ir population (outlined arrow) at a caudal level of the trigeminal motor nucleus showing co-distribution with glutamatergic cells. Note the lateral location of the ascending PmCCK-8-ir tract (arrow). Insets, details of the squared area. **e** Section through the reticular formation showing co-localization with Glu in PmCCK-8-ir cells (outlined arrow). Insets, details of the squared area showing co-localization in some cells (yellow arrowheads). **f** Section through the hypothalamus and details (from a different section in the same region) showing CSF-c PmCCK-8-ir cells co-distributed with GABA-ir cells. **g** Section through the mesencephalon showing perioculomotor PmCCK-8-ir cells (outlined arrow) close to the M3 cell (note the unspecific stained nucleus of the M3 cell). Insets, detail of the squared area showing co-distribution with GABA-ir cells. **h** Lateral CCK-ir population (outlined arrow) at the level of the facial motor nucleus showing co-localization with GABA. Insets, details of the squared area showing co-localization in some cells (yellow arrowheads). **i** Section through the caudal reticular region showing co-location of PmCCK-8 and GABA in two small neurons (outlined arrow). Insets, details of the squared area showing double-labelled cells (yellow arrowheads). The blue channel (**b**–**i**) represents bisbenzimide nuclear stain. For abbreviations, see the list. Dorsal is to the top. Scale bars = 50 µm

PmCCK-8-ir fibres are fairly abundant in lateroventral hindbrain regions, but are lacking in the interpeduncular nucleus and are scarce in ventromedial reticular regions and in the octavolateralis area, trigeminal descending nucleus, and dorsal column nucleus (Figs. 3k–q, 13h, i).

Further characterization of PmCCK-8-ir neuronal populations by double immunofluorescence and tract-tracing methods

For further characterization of the PmCCK-8-ir neurons and to clarify their relation with other systems, we performed double immunofluorescence of PmCCK-8 and some neurotransmitters (GABA, Glu, 5-HT), neuropeptides (NPY-like), or neurotransmitter synthesizing enzymes (TH) (Figs. 9, 10, 12). Most of these experiments were done in larvae. We also performed PmCCK-8 immunohistochemistry combined with tract-tracing from the spinal cord in larvae (Fig. 14).

Glutamate and PmCCK-8

Glutamatergic neuronal populations are abundant in the brain of sea lamprey larvae (Villar-Cerviño et al. 2011, 2013), including cells in most regions containing PmCCK-8-ir cells. For investigating possible co-localization, we analysed sections of larval brains double immunostained for PmCCK-8 and Glu. In the ventral hypothalamus, abundant PmCCK-8-ir and Glu-ir CSF-c neurons are intermingled in the periventricular cell layer (Fig. 9a). Close inspection revealed that PmCCK-8 and Glu immunoreactivities are largely located in different perikarya, as well as in different intraventricular club endings, indicating that they form separated populations. Similar results (no co-localization) were obtained in the PmCCK-8-ir populations of the posterior tubercle (Fig. 9b), nucleus of the medial longitudinal fasciculus, midbrain, and the hindbrain lateral region associated with the trigeminal (Fig. 9d) and facial motor nuclei. Instead, in the medial part of the posterior rhombencephalic reticular nucleus, double immunofluorescence revealed that most PmCCK-8-ir cells were also Glu-ir (Fig. 9e). Interestingly, double immunofluorescence in larval brains revealed that the characteristic longitudinal tract of CCK-ir fibres of the hindbrain coursing towards the dorsal isthmus ends on a compact periventricular population of Glu-ir perikarya (Fig. 9c).

We also investigated possible co-localization of Glu and PmCCK-8 in young adult brains. A number of PmCCK-8-ir neurons of the ventral hypothalamus showed co-localization with Glu immunoreactivity in young adults (Fig. 12a). In the hindbrain, co-localization was observed in cells of the dorsal isthmic PmCCK-8-ir population of young adult brains (Fig. 12b), which was not present in larvae. A proportion of these PmCCK-8-ir neurons showed Glu immunoreactivity. Interestingly, the location of this double-labelled cell population appears to correspond with the above-mentioned Glut-ir periventricular populations receiving conspicuous CCKergic innervation in larvae. More caudally in the hindbrain, Glu/CCK co-localization was observed in small cells of the reticular region similar to those observed in larvae (Fig. 12c).

GABA and PmCCK-8

GABA-ir neurons are widely distributed in the brain of the sea lamprey (Meléndez-Ferro et al. 2002, 2003; Robertson et al. 2007; Villar-Cerviño et al. 2008, 2009). We investigated the possibility of co-localization of GABA in PmCCK-8-ir neurons of the different larval brain regions where co-distribution was noted using double immunofluorescence and confocal microscopy. In the hypothalamus, numerous GABA-ir CSF-c cells are observed in the periventricular region containing PmCCK-8-ir neurons. However, no co-localization of PmCCK-8 and GABA in these neurons was observed, and PmCCK-8-ir perikarya were in general located outwardly to GABA-ir cells in the cell layer (Fig. 9f). Similar results (co-distribution of GABA-ir and PmCCK-8-ir neurons but no co-localization in cells) were observed

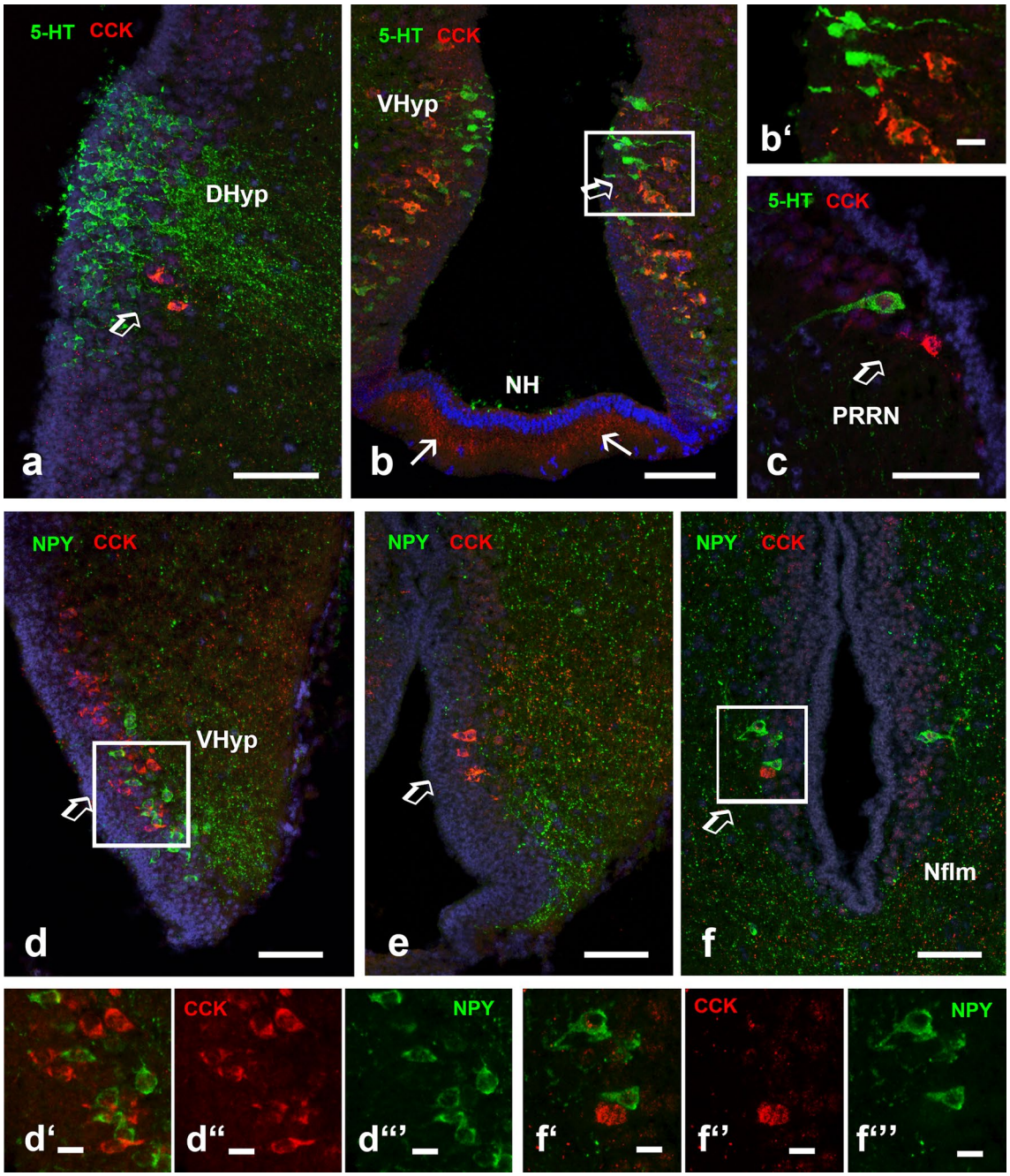

Fig. 10 Confocal photomicrographs of double immunostained sections of larval brains showing PmCCK-8-ir (CCK, red channel) neuronal populations and co-distribution with serotonergic (5-HT) or NPY-like-ir cells (green channel). **a** Section through the dorsal hypothalamus showing a few PmCCK-8-ir cells (outlined arrow) close to a large population of serotonergic CSF-c cells. **b** Section through the hypothalamus at the level of the neurohypophysis. Note abundant PmCCK-8-ir fibres in the neurohypophysis (thin arrows). **b′** Detail of the squared area in b showing co-distribution of PmCCK-8-ir and 5-HT-ir cells. **c** Section through the posterior hindbrain reticular region showing co-distribution of 5-HT-ir and PmCCK-8-ir cells. **d**–**d‴**, section and details (squared area) of the ventral hypothalamus showing co-distribution of NPY-ir and PmCCK-8-ir neurons (outlined arrow). **e** Section of the caudal hypothalamus showing periventricular PmCCK-8-ir cells (outlined arrow) and numerous PmCCK-8-ir and NPY-ir processes in the lateral neuropil. **f**, **f‴** Section and details (squared area) of the nucleus of the medial longitudinal fasciculus (outlined arrow) showing co-distribution of some NPY-ir and PmCCK-8-ir neurons. The blue channel (**a**–**f**) represents bisbenzimide nuclear stain. For abbreviations, see the list. Dorsal is to the top. Scale bars = 50 µm (**a**–**f**), 10 µm (**b′**, **d′**–b‴, **f′**–**f‴**)

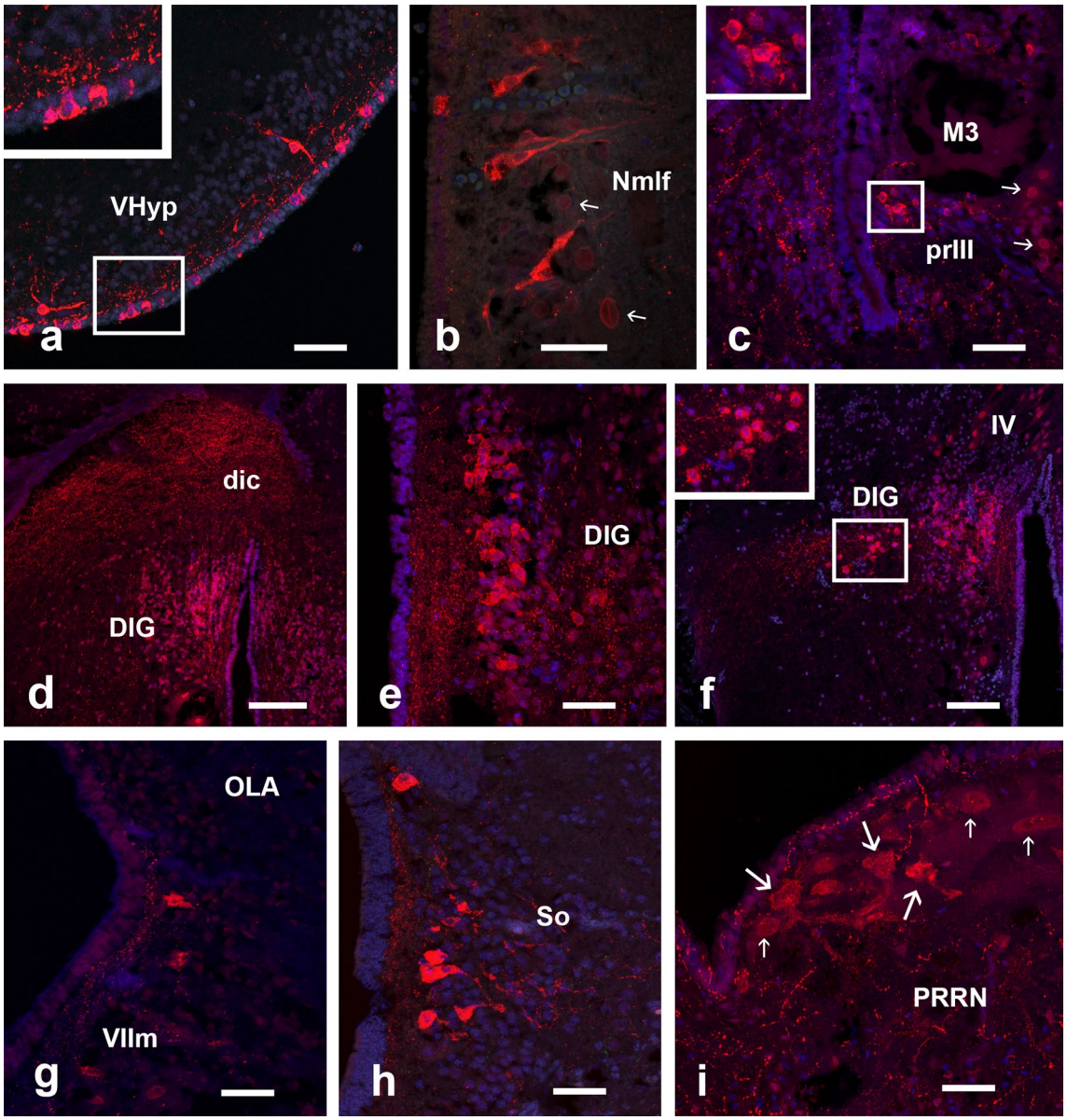

Fig. 11 Confocal photomicrographs of sections of adult lamprey brains showing PmCCK-8-ir (red channel) neuronal populations. **a** Photomicrograph and detail (squared area, inset) of PmCCK-8-ir neurons of the ventral hypothalamus. **b** PmCCK-8-ir neurons in the nucleus of the medial longitudinal fasciculus. Small arrows point to faintly stained cell nuclei of large cells. **c** Photomicrograph and detail (squared area, inset) of perioculomotor PmCCK-8-ir neurons below the M3 giant cell. Small arrows point to nuclei of oculomotoneurons. Panoramic view (**d**) and details of the dorsal isthmus showing PmCCK-8-ir cells in the medial region (**d**, **e**) and extending laterally (**f**, see a detail of the squared area in the inset) and numerous fibres coursing in the dorsal isthmic commissure (dic) and in the dorsal isthmic grey (DIG). **g** PmCCK-8-ir cells in the region lateral to the facial motor nucleus. **h** Section through the intermedio-lateral region of the caudal hindbrain showing numerous PmCCK-8-ir cells in the putative nucleus of the solitary tract. **i** Section through the medial part of the posterior reticular region showing PmCCK-8-ir cells (large arrows). The small arrows point to non-specific staining of the nuclei of larger reticular cells. The blue channel **a**–**f** represents bisbenzimide nuclear stain. **c**–**h** are photomicrographs of sections from young adults, **a**, **b** and **i** from a mature upstream-migrating lamprey. For abbreviations, see the list. Dorsal is to the top. Scale bars = 50 µm (**a**, **b**, **c**, **e**, **g**–**i**), 100 µm (**d**, **f**)

in the posterior tubercle, nucleus of the medial longitudinal fasciculus, and midbrain PmCCK-8-ir populations of larvae (Fig. 9g). Interestingly, double immunofluorescence in the caudal region of the trigeminal motor nucleus and the facial motor nucleus showed partial co-localization of GABA in PmCCK-8-ir neurons: some small lateral reticular cells associated with the visceromotor column were GABA-ir/PmCCK-8-ir, while other cells were either only

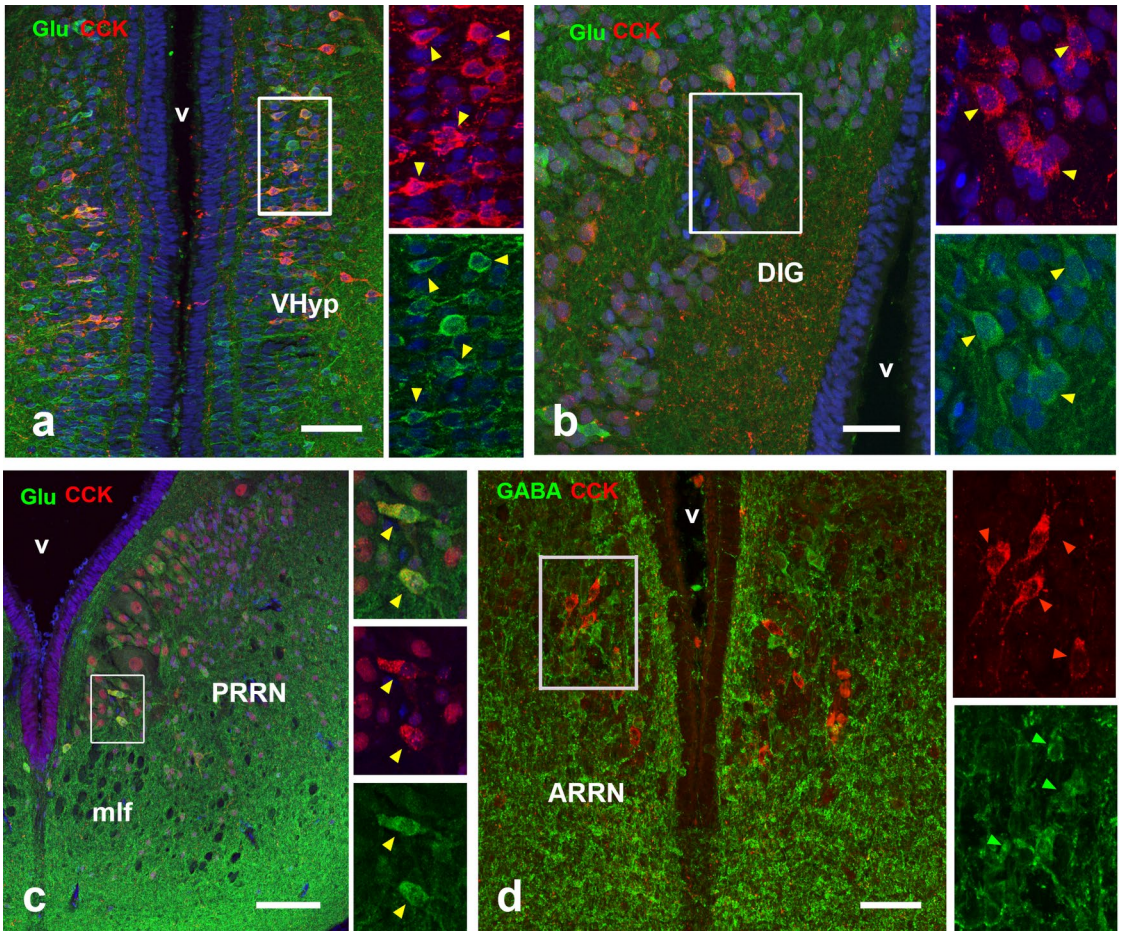

Fig. 12 Confocal photomicrographs of double immunostained sections of adult lamprey brains showing in **a**–**c** co-localization of Glu (green channel) and PmCCK-8 in some cells and in **d** co-distribution of GABA-ir neurons (green channel) and PmCCK-8 neurons (red channel). **a** Photomicrograph and details (squared area) showing co-localization of PmCCK-8 and Glu in CSF-c neurons of the ventral hypothalamus. **b** Photomicrograph and details (squared area) showing co-localization of PmCCK-8 and Glu in periventricular neurons of the dorsal isthmic grey. **c** Section and details (squared area) through the posterior reticular region showing some double labelled small PmCCK-8-ir cells (yellow arrowheads). Cell nuclei show weak autofluorescence signal in the red channel. **d** Section through the ventral isthmus showing that small PmCCK-8-ir cells (red arrowheads in upper detail) are not GABA-ir. Note single-stained GABA-ir cells (green arrowheads in lower inset). The blue channel (**a**–**c**) represents bisbenzimide nuclear stain. For abbreviations, see the list. Dorsal is to the top. Scale bars = 50 µm (**a**, **d**), 25 µm (**b**), 100 µm (**c**)

PmCCK-8-ir or GABA-ir (Fig. 9h). Moreover, PmCCK-8-ir cells of this region appear to give rise to fibres coursing to the dorsal isthmic grey. Here, some of the PmCCK-8-ir fibres ending on the isthmic periventricular population were doubly labelled with the anti-GABA antibody (not shown). In the medial reticular formation of the posterior hindbrain, a few small reticular cells were also GABA-ir/PmCCK-8-ir (Fig. 9i).

We also investigated possible co-localization of GABA in PmCCK-8-ir isthmic populations of young adult brains that were not present in larval brains. These isthmus PmCCK-8-ir neurons did not show GABA immunoreactivity (Fig. 12d).

Serotonin (5-HT) and PmCCK-8

In larval sea lamprey brains, some PmCCK-8-ir neurons were observed in hypothalamic and hindbrain regions containing 5-HT-ir neurons (Abalo et al. 2007; Barreiro-Iglesias et al. 2009a; Cornide-Petronio et al. 2013). Double immunofluorescence in the hypothalamus revealed that 5-HT-ir and PmCCK-8-ir cells are partially co-distributed, but no double-labelled neuron was observed in this region (Fig. 10a, b). In general, PmCCK-8-ir cells occupied outer parts of the periventricular cellular region, whereas 5-HT-ir perikarya were closer to the ventricle. Both types of cells showed ventricular processes ending in small intraventricular clubs (i.e., CSF-c cells). In the dorsal hypothalamus, the number of 5-HT-ir cells is higher than that of PmCCK-8-ir cells. In the

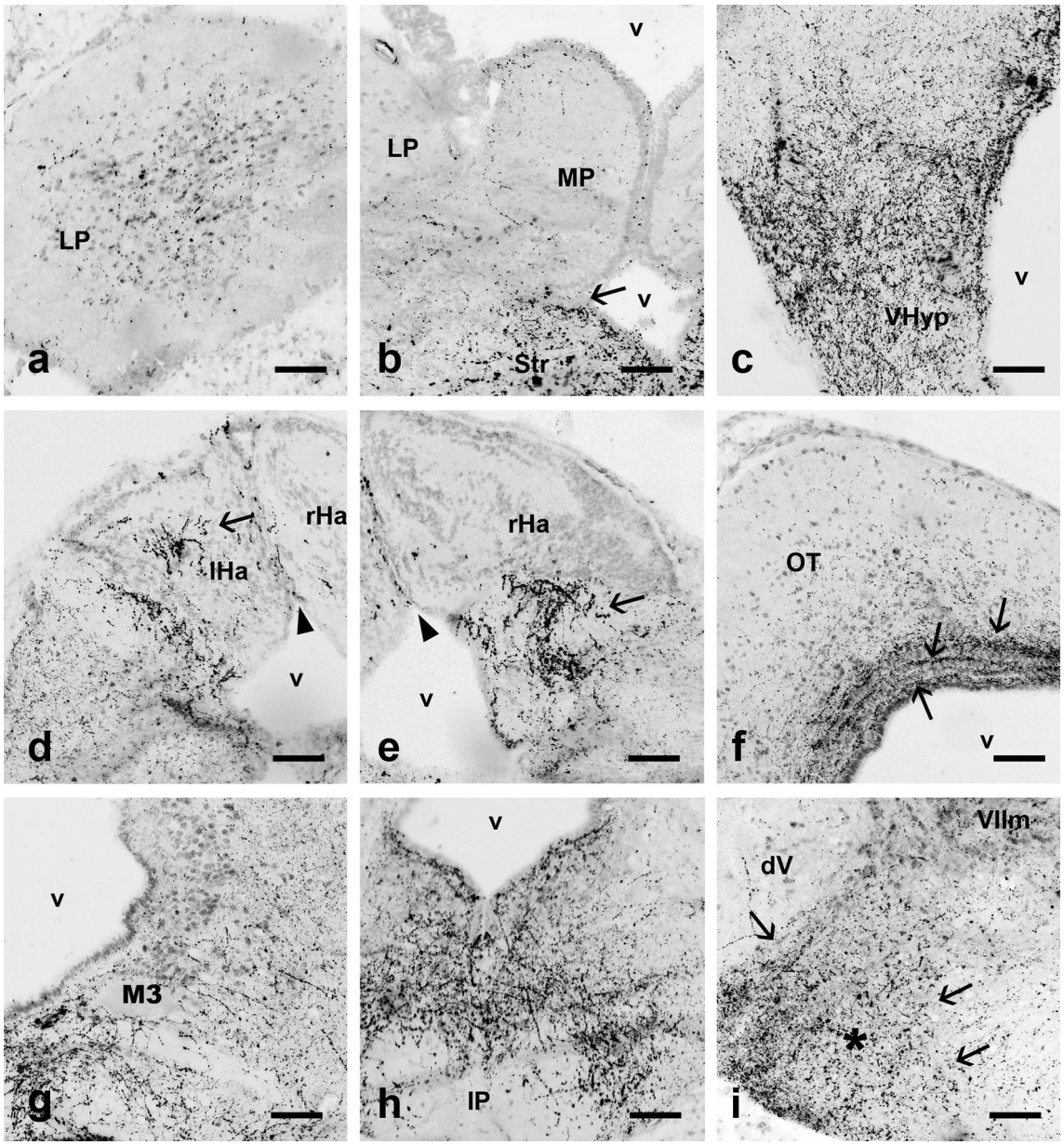

Fig. 13 Fluorescence photomicrographs showing the distribution of PmCCK-8-ir fibres (in black) in selected transverse sections of the brain of a young adult. **a** Tangential section through the caudal pallial hemisphere. **b** Section showing the different fibre densities in the striatum and medial and lateral pallium. **c** Section showing the high density of fibres in the hypothalamus at caudal levels and close the neurohypophysis. **d**, **e** Sections through caudal levels of the left and right habenulas showing the regions with rich innervation (arrows). Arrowheads point to the interhabenular sulcus. **f** Section of the optic tectum showing thin layers of PmCCK-8-ir fibres (arrows) in the periventricular grey and scarce fibres in outer region. **g** Section showing fibres in the midbrain tegmentum. **h** Section of the ventro-rostral isthmus showing rich PmCCK-8-ir innervation in regions dorsal to the interpeduncular nucleus. **i** Section through the region ventrolateral to the facial motor nucleus showing the conspicuous longitudinal tract of PmCCK-8-ir fibres (asterisk, arrows). Colour photomicrographs were transformed to grey scale, and inverted and adjusted for brightness and contrast. Note that in fluorescence photomicrographs taken with a wide band filter, neurons show faint red autofluorescence seeming pale grey. For abbreviations, see the list. Dorsal is to the top. Scale bars = 100 µm

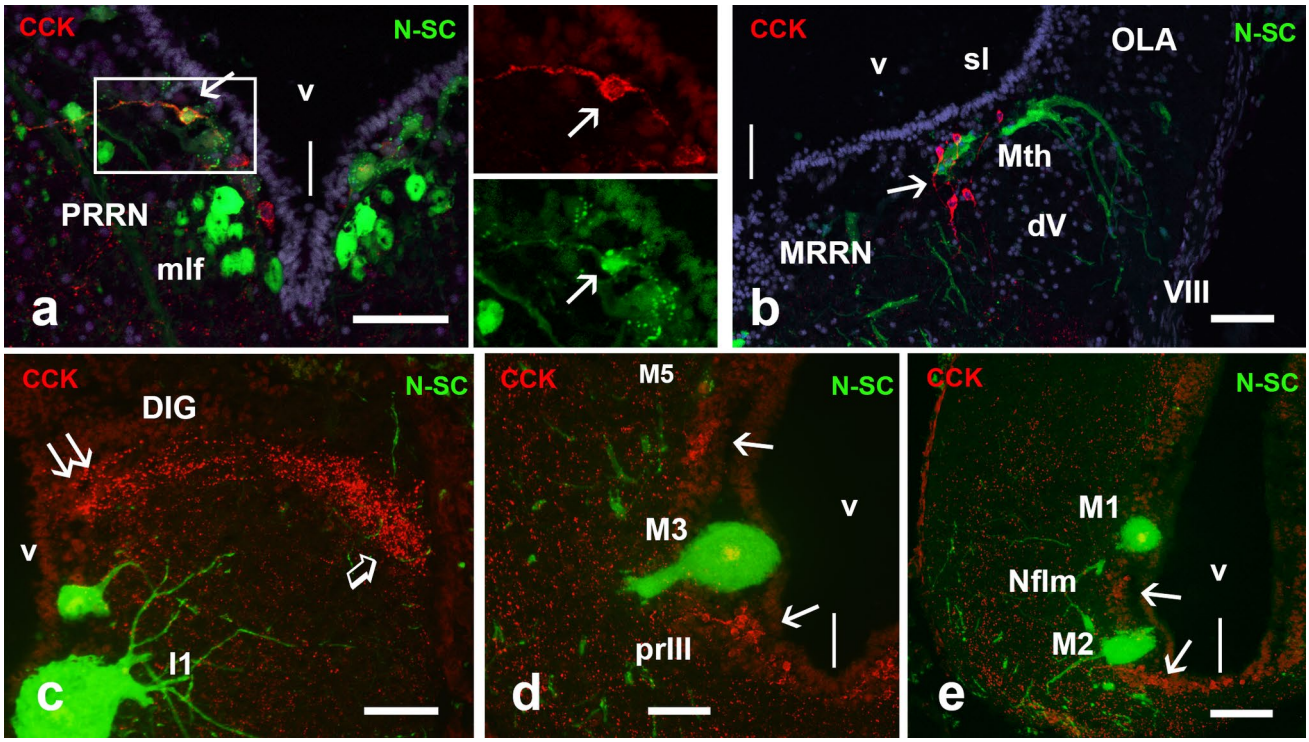

Fig. 14 Confocal (**a**, **b**, **e**) and fluorescence photomicrographs (**c**, **d**) of transverse sections of brains of experimental larvae injected with neurobiotin in the spinal cord (SC) and immunostained with the PmCCK-8 antibody. **a** Section through the posterior reticular region showing a retrogradely labelled PmCCK-8-ir cell (arrow and detail in the inset). Note the thick diameter of mlf axons. **b** Group of PmCCK-8-ir cells (arrow) close to the lateral dendrite of a Mauthner cell. **c** Section through the isthmus showing the projection of a conspicuous PmCCK-8-ir tract (outlined arrow) on a periventricular nucleus (double arrow) that is dorsal to big retrogradely labelled reticular neurons. **d** Section through the midbrain tegmentum showing PmCCK-8-ir cells (arrows) that lie dorsal and ventral to the labelled M3 cell. **e** Section through the caudal diencephalon showing the relation of PmCCK-8-ir cells (arrows; nucleus of the medial longitudinal fasciculus) to the labelled giant M1 and M2 cells. The vertical bars (**a**, **b**, **d**, and **e**) indicate the midline. For abbreviations, see the list. Dorsal is to the top. Scale bars = 50 µm (**a**, **b**), 100 µm (**c**, **d**), 200 µm (**e**)

caudal hindbrain of larvae, small 5-HT-ir cells and PmCCK-8-ir cells are co-distributed in the medial region over the medial longitudinal fasciculus, but again, no double-labelled cells were observed (Fig. 10c).

PmCCK-8 and neuropeptide Y (NPY)

In larvae, some PmCCK-8-ir neurons are located in brain regions containing NPY-like-ir neurons, such as the ventral hypothalamus and posterior tubercle (Barreiro-Iglesias et al. 2010b). Double immunofluorescence for PmCCK-8 and NPY showed no co-localization of both substances in the ventral hypothalamus, although NPY-like-ir and PmCCK-8-ir cells are numerous and appear partially co-distributed (Fig. 10d, e). In the posterior tubercle and nucleus of the medial longitudinal fasciculus, NPY-like-ir cells are located close but dorsal to the U-shaped band of PmCCK-8-ir cells (Fig. 10f). The NPY-like-ir cells observed in the dorsal isthmus were ventral to the periventricular region innervated by PmCCK-8-ir fibres (not shown).

PmCCK-8 and tyrosine hydroxylase (TH)

We investigated possible co-localization of PmCCK-8 and TH immunoreactivities in adult brain regions that show both TH-ir (dopaminergic) (hypothalamus, posterior tubercle; see Barreiro-Iglesias et al. 2010a) and CCK-ir (present results) cells. No co-localization of CCK and TH immunoreactivity was observed in cells of these populations (not shown).

Spinal cord PmCCK-8-ir fibres and tract-tracing in larval lampreys

Since *PmCCK* + or PmCCK-8-ir perikarya were not observed in the spinal cord, we hypothesized that spinal PmCCK-8-ir fibres must originate from brain neurons. To identify the cells of origin of these fibres, we applied neurobiotin to the larval spinal cord at the level of the fifth branchial cleft. After appropriate transport time, brain sections were immunostained for PmCCK-8 and then were analysed for the presence of neurobiotin. This procedure led to the neurobiotin labelling of well-characterized populations

of brain–spinal neurons, which are distributed from the diencephalon to the hindbrain (McClellan 1992; Barreiro-Iglesias et al. 2008a, b; Cornide-Petronio et al. 2011). Of the various neurobiotin-labelled brain–spinal projection neurons co-distributing with PmCCK-8-ir cells (Fig. 14a–e), only a few small cells in the medial reticular region of the caudal hindbrain were double labelled with PmCCK-8, pointing to this population as the origin of PmCCK-8-ir spinal fibres (Fig. 14a). These tract-tracing experiments also revealed the location of some trigeminal-facial PmCCK-8-ir neurons close to the lateral dendrite of the retrogradely labelled Mauthner neuron (Fig. 14b), and the location of small PmCCK-8-ir cells with regards to diencephalic and mesencephalic giant Müller cells (Fig. 14d, e). Dendrites of these giant neurons branch in regions containing numerous PmCCK-8-ir fibres, suggesting that they may receive contacts from these fibres. In the isthmus, experiments reveal the location of the main target of the PmCCK-8-ir tract dorsal to the group of large isthmic reticulospinal neurons and also show that dendrites of these large cells course in a region rich in PmCCK-8-ir fibres (Fig. 14c).

Presence of PmCCK-8-ir neuroendocrine cells in the larval sea lamprey gut

Some gut samples from larval lamprey were processed for immunofluorescence with the PmCCK-8 antibody. These samples included the intestine with the typhlosole. Slender bipolar PmCCK-8-ir cells extended radially throughout the height of the intestinal epithelium (not shown), confirming the presence of cholecystokininergic endocrine cells (Van Noorden and Pearse 1974).

Discussion

Identification of a CCK-type precursor in the sea lamprey

Here, we report the cloning and sequencing of a cDNA encoding the *PmCCK* precursor. Although we also searched for a gastrin precursor sequence in available sequence data for *P. marinus*, this search did not reveal any sequences resembling gastrin precursors from jawed vertebrates. Since both CCK and gastrin genes have been reported in all jawed vertebrate groups investigated so far (Roelants et al. 2010), our results suggest that the gene duplication that gave rise to these two genes may have occurred after the separation of jawless and jawed fishes, although other possibilities cannot be ruled out (e.g., that the gastrin gene was lost in extant agnathans). Analysis of the PmCCK precursor protein sequence predicts the presence of a 22 amino acid N-terminal signal peptide, a dibasic cleavage site in the C-terminal region and a tyrosine sulfation site in the mature PmCCK-8 peptide. The pro-peptide is 146 residues in length, which is in the upper range of lengths of CCK pro-peptides reported in other vertebrates. The lengths of CCK-type precursor proteins predicted from reported gene sequences (searched in GenBank) are 114–115 residues in most eutherian mammals, 126–129 residues in metatheria, 122–130 residues in reptiles, 129–130 residues in birds (Lovell and Mello 2011) and 128–130 residues in frogs. The predicted sequences of the two or more precursor CCKs reported in teleosts are more variable in length, ranging from 117 to 138 residues (GenBank), while in cartilaginous fishes, the reported CCK-type precursor sequences are between 125 and 130 residues (GenBank). Comparison of the sequence of the C-terminal region of PmCCK with this region of CCK-type precursors from other vertebrates (including another lamprey species) revealed high conservation of the CCK-8 motif, with only a single amino acid change in the third position in lampreys by comparison with the CCK-8 sequence reported in mammals, other tetrapods, and elasmobranchs. Sequence variations in this third position and duplications of the CCK gene found in teleosts are probably derived characteristics (Kurokawa et al. 2003; Roelants et al. 2010). Furthermore, based on the presence of putative cleavage sites, the existence of longer isoforms of CCK in the sea lamprey is predicted.

Comparison of the complete CCK precursor sequences allowed the reconstruction of a phylogenic tree, the topology of which is generally in agreement with chordate phylogeny. In the tree, the CCK precursors of lampreys are closely related and form an out-group to all gnathostome precursors, which divide into chondrichthyan and osteichthyan (bony fishes and land vertebrates) clades. However, the structure of the osteichthyan clade of the tree, with mammalian sequences not clustering with other tetrapod sequences, may be influenced by variation in preprotein lengths (for a more detailed tree of CCK precursors from teleosts, see Murashita et al. 2009).

Biochemical studies using radioimmunoassay methods to analyse gut and brain extracts and immunochemistry using anti-CCK antibodies with different affinities indicated the possible existence of two or more CCKs in lampreys (Holmquist et al. 1979; Van Dongen et al. 1985), although these "CCKs" were never identified. The major CCK-like component detected by radioimmunoassay was similar, but not identical, to the C-terminal fragments of mammalian CCK precursors (Holmquist et al. 1979), which may be due to the differences in the sequences of PmCCK-8 and mammalian CCK-8 reported here. Our analysis of the sea lamprey CCK precursor sequence clearly indicated the presence of a 22-residue signal peptide and predicted a highly probable dibasic cleavage site. Sequence comparison with CCKs from other vertebrates also revealed the presence of a highly conserved monobasic cleavage site. Cleavage at these

sites would generate the PmCCK-8 peptide, which may be the main product of CCK pro-peptide processing in the sea lamprey. In addition, sequence analyses also revealed the presence of a tyrosine sulfation site, which suggests that sulfated PmCCK-8 is the main mature peptide in the CNS of lampreys, as in other vertebrates (Agersnap et al. 2016). Accordingly, we observed strong immunoreactivity in the sea lamprey CNS with an antibody generated against the sulfated version of PmCCK-8 (see below).

Cholecystokinergic neurons in the sea lamprey brain

The anatomical distribution of CCK, neuropeptide Y (NPY), and galanin, which have central effects on feeding in mammals, has been reported in lampreys (Jiménez et al. 1996; Brodin et al. 1988; Barreiro-Iglesias et al. 2010b; present results). In mammals, injection of NPY and galanin has orexigenic effects, whereas CCK suppresses feeding (Lee et al. 1994). In lamprey brains, these peptides show different distributions. Thus, galanin-like-ir perikarya are largely restricted to the hypothalamus and thalamus, although fibres are distributed throughout most brain regions (Jiménez et al. 1996). In contrast, the brain distribution of both NPY and CCK neurons is more widespread, but in only a few regions (hypothalamus, posterior tubercle, and lateral reticular region), these neurons are co-distributed and important regional differences in their populations were noted (Brodin et al. 1988; Barreiro-Iglesias et al. 2010b; present results). Moreover, the distribution of fibres immunoreactive for NPY and CCK also show important differences in various brain regions. This suggests that these peptides are differentially involved in various neural circuits of the sea lamprey.

Previous studies of the cholecystokinergic system of lampreys were centred on the expression of CCK-like peptides in the reticular formation (Brodin et al. 1988), and in the functional analysis of CCK in spinal circuits (van Dongen et al. 1985; Buchanan et al. 1987; Ohta et al. 1988; Parker 2000). Our analysis in the sea lamprey brain with ISH using a probe for the *PmCCK* precursor reveals the presence of neurons expressing *PmCCK* mRNA in populations of neurons in the hypothalamus, posterior tubercle, prethalamus, the nucleus of the medial longitudinal fasciculus, midbrain tegmentum, isthmus, rhombencephalic reticular formation, and the putative nucleus of the solitary tract. Moreover, comparison of *PmCCK* expression in larvae and adult sea lampreys indicates that some populations of *PmCCK*-positive neurons are only observed in adults, highlighting notable differences between the cholecystokinergic systems of larvae and adults. We also investigated this system using an antibody raised specifically against the PmCCK-8 peptide, which allowed further characterization of the sea lamprey cholecystokinergic system by revealing both perikarya and processes. Evidence of the antibody specificity is provided by the similar distribution of neurons exhibiting PmCCK-8-ir and neurons expressing the *PmCCK* precursor mRNA as revealed by ISH, including similar differences between larvae and adults. Some of these PmCCK-8-ir populations (posterior and middle rhombencephalic reticular nuclei, mesencephalic reticular nucleus, and hypothalamus) have been reported previously in adults of other lamprey species (*Lampetra fluviatilis* and *Ichthyomyzon unicuspis*) using various anti-mammalian CCK antibodies (Brodin et al. 1988), but not the other *PmCCK* cell groups reported here. The finding in adult lampreys that a preoptic population exhibits immunoreactivity to the PmCCK-8 antibody, but does not express *PmCCK* mRNA, could be explained by low transcript abundance in this population.

Comparisons with other vertebrates

Telencephalon

The telencephalon of mammals contains numerous CCK-positive neurons, mainly in the pallium (Burgunder and Young 1990b; Tohyama and Takatsuji 1998), and abundant CCK-positive populations have been also reported using ISH in the pallium of birds (Maekawa et al. 2007; Lovell and Mello 2011). The CCK-positive neurons of the pallium are part of intracortical circuits, adding to thalamo-cortical CCK-positive circuits (Burgunder and Young 1988, 1990a). For instance, in the telencephalon of birds, CCK is involved in higher neural functions such as imprinting after hatching (Maekawa et al. 2007) or song regulation (Lovell and Mello 2011). Instead, no CCK peptide or mRNA expression has been reported in cells of the pallium of frogs (Petkó and Kovács 1996; Rourke et al. 1997), and some teleosts (Batten et al. 1990; Murashita et al. 2009), which represents a significant difference with the pallium of amniotes. Although mRNA expression of two CCKs is prominent in the telencephalon of the rainbow trout (Jensen et al. 2001) and flounder (Kurokawa et al. 2003), these authors did not investigate the regional expression. In the sea lamprey, no PmCCK expressing cells were observed in the pallium or subpallium with IHC or ISH (present results). This represents a difference with teleosts and frog, which show CCK-ir cells in the ventral telencephalic area (*Poecilia*: Batten et al. 1990; goldfish: Himick and Peter 1994; frog: Petkó and Kovács 1996). In *Lampetra fluviatilis*, Suryanarayana et al. (2017) also noted the absence of CCK-like-ir cells in the pallium. Other important differences among vertebrates are related with the presence of CCK-positive perikarya in the olfactory bulb of mammals (Ingram et al. 1989; Tohyama and Takatsuji 1998; Gutièrrez-Mecinas et al. 2005). High CCK mRNA levels were detected in the goldfish olfactory

bulb (Peyon et al. 1999). However, no CCK-positive neurons were observed in the sea lamprey olfactory bulb, suggesting that this peptide is not involved in olfactory functions.

Preoptic region and hypothalamus

The preoptic area and the hypothalamus (supraoptic and paraventricular nuclei, dorsomedial hypothalamic nucleus) of mammals contain numerous CCK-ir neurons (Vanderhaeghen et al. 1980; Tohyama and Takatsuji 1998; Crosby et al. 2015). The dorsomedial hypothalamic nucleus is a region implicated in satiety and stress control. It is known that application of exogenous CCK modulates food intake and neuropeptide expression (Crosby et al. 2015). CCK also exerts actions over oxytocinergic neurons of the paraventricular nucleus (Cano et al. 2003). In birds, intraventricular CCK application inhibits feeding and also exerts effects (activation of Fos-like immunoreactivity) on nuclei of the hypothalamus (Boswell and Li 1998). In the preoptic region and the hypothalamus of teleosts, the presence of CCK-ir perikarya was reported in the entopeduncular nucleus, preoptic nucleus, anterior or posterior periventricular nucleus, lateral recess nucleus, and lateral tuberal nucleus (*Poecilia*: Batten et al. 1990; goldfish: Himick and Peter 1994). This is consistent with the finding that the highest CCK mRNA levels of the goldfish brain were detected in the hypothalamus (Peyon et al. 1999). In goldfish, intraperitoneal injection of CCK-8 significantly decreased feeding relative to saline-injected controls (Himick and Peter 1994). In the rainbow trout, Jensen et al. (2001) also reported CCK mRNA expression in the saccus vasculosus, a neurovascular structure present in elasmobranches and in some bony fishes but not in lampreys and tetrapods. Our results in the sea lamprey did not reveal *PmCCK* mRNA expression in neurons of the preoptic region, but we found abundant expression in three hypothalamic nuclei, the ventral and dorsal hypothalamic nuclei, and the nucleus of the postoptic commissure, which exhibit notable differences among them in cell size and *PmCCK* expression. The first two nuclei comprise PmCCK-8-positive CSF-c neurons, a cell type that has been reported in the posterior periventricular nucleus of the goldfish (Himick and Peter 1994). The possible functional significance of these lamprey hypothalamic populations in relation to feeding control has not been investigated yet, but our results reveal that PmCCK-8 is strongly expressed in the ventral and dorsal hypothalamic populations of non-feeding adults, judging both the intensity of the *PmCCK* hybridization signal and PmCCK-8 immunoreactivity. Adult sea lampreys at the stages investigated (young animals caught in the river prior to downstream migration to the sea and the mature upstream-migrating adults) do not feed, so we speculate that the abundance of PmCCK-8 in hypothalamic nuclei might be related to feeding inhibition in these stages. How CCK expression in the larval hypothalamus is related to the filter-feeding behaviour needs also be investigated.

Posterior tubercle

PmCCK-expressing neurons are observed in the ventral region of the posterior tubercle of the sea lamprey, both in larvae and adults, from where CCK-positive populations extend to the midbrain tegmentum. In lampreys, the posterior tubercle contains dopaminergic populations that project to the striatum (Pombal et al. 1997), whereas dopaminergic populations are lacking in the caudal diencephalon and mesencephalic tegmentum (Pombal et al. 1997; Pierre et al. 1997; Barreiro-Iglesias et al. 2010a). It has been hypothesized that posterior tubercle dopaminergic populations of lampreys and teleosts are functionally equivalent to the ventral tegmental area/substantia nigra midbrain dopaminergic populations that project to the basal telencephalon in mammals (Pombal et al. 1997; Rink and Wullimann 2002), and recently, this dopaminergic population in lampreys was named "substantia nigra pars compacta" (Stephenson-Jones et al. 2012; Pérez-Fernández et al. 2014), although the homonymous mammalian nucleus mainly originates in the mesencephalic tegmentum (Hayes et al. 2011; Panman et al. 2014). In mammals, CCK immunoreactivity is co-expressed in some dopaminergic neurons of the ventral tegmental area and CCK and dopamine are co-released on their telencephalic targets (Jayaraman et al. 1990). There, CCK modulates dopamine release and dopamine-mediated reward, which has major implications for neurologic and psychiatric diseases (Beinfeld 2001). Our results in the sea lamprey do not reveal PmCCK-8 immunoreactivity in dopaminergic (TH-positive) neurons of the hypothalamus/posterior tubercle, which suggests that rewarding circuits of the basal forebrain of lampreys and mammals differ with regard to the use of CCK.

Thalamus

The thalamus (dorsal thalamus) contains numerous CCK-expressing neurons in mammals (Voigt and Uhl 1988; Burgunder and Young 1988, 1989a; De Belleroche et al. 1990; Senatorov et al. 1997; Giacobini and Wray 2008) and birds (Lovell and Mello 2011; Wang et al. 2017). In mammals, CCK cells of the auditory thalamus and cerebral cortex are reciprocally connected and might be involved in seizure genesis (Senatorov et al. 1997). *PmCCK*-expressing neurons have been observed in the prethalamus (ventral thalamus) of lamprey (present results) and CCK-ir cells are also present in the ventral thalamus of the green molly (Batten et al. 1990). This suggests that the prethalamic CCK expression

is a shared feature in fishes, although the projections and function of these prethalamic cells are not known.

Habenula

The innervation of the sea lamprey habenula by PmCCK-8-ir fibres is very selective, ending on the ventral region of the right habenula and on the left habenula. These two habenular regions are considered the homologue of the mammalian medial habenular nucleus (Stephenson-Jones et al. 2012). In rats, CCK-ir fibres also innervate the medial habenular nucleus, but not the lateral habenular nucleus (Tohyama and Takatsuji 1998). The present findings in the lamprey habenula add to other findings showing a similar pattern of alpha-transducin fibre innervation of the medial habenular nucleus homologue. These findings indicate the presence of direct CCK-ir pathways probably originating from hypothalamic or posterior tubercle populations, projecting selectively onto this habenular region. These projections were not noted by other studies (Yáñez and Anadón 1994; Stephenson-Jones et al. 2012; Grillner et al. 2018).

Midbrain

Optic tectum No *PmCCK*-expressing perikarya were observed in the sea lamprey optic tectum. This absence of tectal CCK-expressing neurons contrasts with the abundance of CCK mRNA-expressing cells reported in the optic tectum of some teleosts (rainbow trout: Jensen et al. 2001; flounder: Kurokawa et al. 2003). CCK expression was also reported by ISH in cells of the frog tectum (Rourke et al. 1997), although not with immunohistochemistry (Petkó and Kovács 1996). In the optic tectum of the adult sea lamprey, PmCCK-8-ir fibres were rather abundant, mostly in deep tectal layers. With regard to other vertebrates, the presence of CCK-ir fibres has been reported in the optic tectum of teleosts (Himick and Peter 1994), frogs (Petkó and Kovács 1996), and rat (superior colliculus: Kubota et al. 1983; Tohyama and Takatsuji 1998), suggesting that CCK is involved in modulation of tectal circuits of these vertebrates. Interestingly, there is a notable difference between adult lampreys and larval lampreys, which mostly lack tectal PmCCK-8-ir innervation, a difference probably related to the poor development of the tectum and the retina at this stage (de Miguel and Anadón 1987; de Miguel et al. 1990; Villar-Cerviño et al. 2009, 2013).

Tegmentum The *PmCCK*-expressing neurons of the midbrain tegmentum of the adult sea lamprey form two populations, one more dorsal located in the region of the Schober's M5 nucleus (Schober 1964), which also contains GABAergic neurons (Meléndez-Ferro et al. 2002; Robertson et al. 2006) and another more ventral. Cells from the midbrain tegmental region give rise to projections to the optic tectum (Robertson et al. 2006; de Arriba and Pombal 2007), pretectum (Capantini et al. 2017), and retina (Vesselkin et al. 1984), which may explain both the rich PmCCK-8-ir innervation of the tectum and the occasional presence of PmCCK-8-ir fibres observed in the adult sea lamprey retina (unpublished observations). In rats, the most densely packed CCK-ir cell population of the brain is found in the periaqueductal grey (Innis et al. 1979) and is probably involved in nociception (Innis and Aghajanian 1986). Midbrain *PmCCK*-expressing populations in the lamprey could correspond to those of the rat periaqueductal grey and might, therefore, have similar physiological roles.

Hindbrain

Dorsal isthmus The adult sea lamprey isthmus contains two populations of *PmCCK*-expressing neurons, one in the dorsal isthmic grey and the other in the ventral reticular region. Considering the absence in the lamprey of a cerebellum comparable to that of gnathostomes (Lannoo and Hawkes 1997), the topology of the dorsal isthmic grey population is probably comparable to the CCK-expressing neuronal populations reported in the lateral parabrachial region of mammals, which project to the hypothalamus (Kubota et al. 1983; Tohyama and Takatsuji 1998; Hermanson et al. 1998). Interestingly, dorsal isthmic cells show *PmCCK* mRNA expression and PmCCK-8-ir only in adult lampreys, either young or upstream migrating. In the isthmus of larvae, we have not found evidence of any of these markers, indicating that in the isthmic region, there is a profound change in *PmCCK* gene expression during transformation. This change in PmCCK-8 expression in these cells may be related to the major changes in feeding biology and head and gut anatomy accompanying the transition from larval to adult lampreys. Major changes in expression of various neuronal markers not observed in larval eyes (opsins, GABA, 5-HT, dopamine, neuropeptides and calcium-binding proteins) have also been reported in the transforming lamprey retina related with the major lifestyle changes occurring during transformation (Anadón et al. 1998; Pombal et al. 2003; Villar-Cerviño et al. 2006; Villar-Cheda et al. 2006, 2008; Abalo et al. 2008; Cornide-Petronio et al. 2015).

Neuronal population lateral to the visceromotor column Immunohistochemical analysis of the larval dorsal isthmus reveals a conspicuous PmCCK-8-ir/GABA-ir tract coursing in the lateral walls of the hindbrain that bends to selectively innervate a glutamatergic neuronal population dorso-rostral to the I1 giant Muller cell. Since this population is located in the same region that in adults contains the dorsal isthmic CCKergic neurons, we hypothesize that these

fibres are contacting isthmic cells that will express PmCCK-8 after transformation. The larval CCK innervation of this neurochemically immature isthmic population appears analogous to the early presence of GABAergic retinopetal fibres in the retina of larvae, which appear to regulate the differentiation state of larval retinal cells before transformation (Anadón et al. 1998). With regard the PmCCK-8-ir tract that contacts the dorsal isthmic grey population in larvae, our immunohistochemical results indicate that the *PmCCK*-expressing neurons accompanying the visceromotor column originate this tract. This population may form part of an ill-defined primary viscerosensory/visceromotor region of the lamprey hindbrain (Koyama 2005). The facial–vagal primary sensory nuclei contain CCK-ir cells in teleosts (Batten et al. 1990; Himick and Peter 1994; Farrell et al. 2002), and the same was reported in the nucleus of the solitary tract of frog (Petkó and Kovács 1996) and rat (Kubota et al. 1983; Hökfelt et al. 1988; Tohyama and Takatsuji 1998). Topographical differences in lamprey CCKergic neuronal populations with regards those of teleosts, frog, and mammals appear to be due to differences in rostrocaudal extension of the viscerosensory column. This column extends caudally from the region of the facial nerve entrance in lampreys, whereas in gnathostome vertebrates, the gustatory/general visceral nuclei occupy a relatively more caudal position in the hindbrain. A similar difference is found with regards the visceromotor column, which is continuous from the level of the trigeminal nerve entrance till the caudal hindbrain in lampreys (Pombal et al. 2001; Pombal and Megías 2019), unlike the discontinuous visceromotor columns found in jawed vertebrates. In any case, the anatomy of the PmCCK-8-ir tract (ventral to the trigeminal descending root) and its target in the dorsal isthmus is reminiscent of the secondary gustatory/visceral tract of teleosts, which projects to a very conspicuous secondary gustatory/visceral nucleus in the isthmus. This teleost nucleus is considered homologous to nuclei of the mammalian parabrachial complex (see Yáñez et al. 2017).

Rhombencephalic reticular formation The presence of CCK-like-ir neurons in the posterior rhombencephalic reticular nucleus has been reported previously in adult lampreys (Brodin et al. 1988, 1989). These authors also found that some of these CCK-ir reticular cells project to the spinal cord and these projections are part of the locomotor circuits (Van Dongen et al. 1985; Ohta et al. 1988; Parker 2000). The present ISH results reveal a column of small-to-medium-sized reticular cells that express *PmCCK* mRNA and are PmCCK-8-ir in both larvae and adults, confirming the cholecystokinergic nature of these cells. Moreover, our double immunohistochemical/tract-tracing experiments in larvae confirm that some of these PmCCK-8-ir neurons have descending projections to the spinal cord. Previous studies have also reported the presence of CCK-ir neurons in the lamprey spinal cord that were immunostained by some of the CCK antibodies used but not with others (Van Dongen et al. 1985; Ohta et al. 1988; Brodin et al. 1988). This led to Brodin et al. (1988) to suggest that some CCK antibodies used in these studies might cross-react with an unknown protein. Here, we were unable to confirm the presence of CCK-ir spinal cells using a specific PmCCK-8 antibody or of *PmCCK* mRNA-expressing cells by ISH, which rules out the presence of intraspinal CCK-expressing cells in the sea lamprey.

In addition to the *PmCCK*-expressing cells of the posterior rhombencephalic reticular nucleus, we have found a population of *PmCCK*-expressing small cells in the ventral isthmo-trigeminal reticular region of the adult sea lamprey. These cells may correspond to those observed in the middle rhombencephalic reticular nucleus of river and silver lampreys by Brodin et al. (1988), although the location of *PmCCK*-expressing cells appears to be more rostral than those reported by these authors and are partially intermingled with 5-HT-ir isthmic cells. The development of the ventral isthmic 5-HT-ir neuronal population in sea lamprey suggests that it corresponds to a raphe nucleus whose cells migrate laterodorsally instead of towards the midline (Abalo et al. 2007), which is unlike the ventral and ventrolateral migration of neurons observed in the formation of raphe nuclei of basal jawed vertebrates (Carrera et al. 2008). CCK mRNA expression was observed in the dorsal raphe nucleus of zebra finch (Lovell and Mello 2011) and CCK-positive neurons were also found in some raphe nuclei of rat (van der Kooy et al. 1981; Mantyh and Hunt 1984; Monti 2010). Unlike the cells of the isthmo-trigeminal region that express serotonin early in sea lamprey larvae (Abalo et al. 2007; Cornide-Petronio et al. 2013), we found no cell in this region expressing *PmCCK-8* in larvae. As indicated above for the dorsal isthmic *PmCCK*-expressing population, the appearance of ventral *PmCCK*-expressing cells in adult lampreys appears to be delayed until metamorphosis when new structures and functions necessary for the adult lifestyle develop.

Co-localization of CCK with other neurotransmitters

GABA and Glu

Well-studied examples of CCK-GABA co-localization in mammals are interneurons of the cerebral cortex, hippocampus and amygdala (McDonald and Pearson 1989; Kubota et al. 1994; Singec et al. 2002; Somogyi et al. 2004). In the cortex, CCK is found in a small percentage of GABAergic interneurons, which are inhibitory (Xu et al. 2010). Since CCK is not expressed in cells of the lamprey telencephalon,

we wondered if a similar co-localization with GABA is found in other PmCCK-8-expressing neurons of the brain. In double immunofluorescence experiments in larval brains, only some cells of the column lateral to the trigeminal and facial motor nuclei were GABA/CCK double-labelled, but co-localization was not observed in the other regions in which CCK cells and GABA-ir cells were co-distributed. To the best of our knowledge, this is the first demonstration of co-localization of GABA and CCK in neurons of a non-mammalian vertebrate. Comparison with mammals indicates that co-localization with GABA is not a general property of CCKergic neurons but of some particular cell types which largely differ between lampreys and mammals. Partial co-localization of GABA with other neurotransmitters (5-HT, dopamine, NPY) in some lamprey brain populations has also been reported (Parker et al. 1998; Rodicio et al. 2008; Barreiro-Iglesias et al. 2009a, b, 2010b).

With regards the distribution of Glu (the main excitatory neurotransmitter in the brain) and CCK, in the brain of larval lampreys, we only found co-localization in cells of the medial nucleus of the posterior reticular formation. Previous studies in sea lamprey showed that vesicular Glu transporter is expressed in many reticular cells of this reticular region (Villar-Cerviño et al. 2013). In addition to the presence of a PmCCK-8/glutamatergic reticular population in the sea lamprey larval brain, the present results in adult lamprey further reveal a PmCCK-8/Glu positive dorsal isthmic population and a population of ventral hypothalamic cells. In mammals, double immunoreactivity to CCK and vesicular Glu transporter 1 (VGluT1) has been reported in numerous axon terminals of the hippocampus in a mouse model with recurrent, spontaneous seizures, indicating that some glutamatergic neurons express CCK (Wyeth et al. 2012). It appears that different GABAergic and glutamatergic populations in the sea lamprey express different combinations of neuropeptides, including CCK, indicating large differences in functional specialization. Unlike in mammals, where these double-labelled populations are mainly found in telencephalic regions involved in higher functions, in the sea lamprey, the double labelled cells appear to form part of more basic hindbrain and hypothalamic circuits, which is a major difference between these animals. It remains to be investigated if similar GABA/CCK or Glu/CCK co-localization occurs in other non-mammalian vertebrates.

Acknowledgements Grant sponsors: Spanish Ministry of Economy and Competitiveness and the European Regional Development Fund 2007–2013 (Grant number: BFU-2017-87079-P). L.A.Y.G was supported by a PhD studentship awarded by the Mexican Council of Science and Technology (CONACyT studentship no. 418612) and Queen Mary University of London. D.R. is supported by Institute Strategic Funding Grants to The Roslin Institute (BBS/E/D/20002172, BBS/E/D/30002275 and BBS/E/D/10002070). The authors thank the staff of Ximonde Biological Station for providing the lampreys used in this study, and the Microscopy Service (University of Santiago de Compostela) and Dr. Mercedes Rivas Cascallar for confocal microscope facilities and help.

Compliance with ethical standards

Conflict of interest The authors declare that they have no conflict of interest (financial or non-financial).

Ethical standards All applicable international, national, and/or institutional guidelines for the care and use of animals were followed.

References

Abalo XM, Villar-Cheda B, Meléndez-Ferro M, Pérez-Costas E, Anadón R, Rodicio MC (2007) Development of the serotonergic system in the central nervous system of the sea lamprey. J Chem Neuroanat 34:29–46

Abalo XM, Villar-Cerviño V, Villar-Cheda B, Anadón R, Rodicio MC (2008) Neurochemical differentiation of horizontal and amacrine cells during transformation of the sea lamprey retina. J Chem Neuroanat 35:225–232

Adám AS, Csillag A (2006) Differential distribution of L-aspartate- and L-glutamate-immunoreactive structures in the arcopallium and medial striatum of the domestic chick (*Gallus domesticus*). J Comp Neurol 498:266–276

Agersnap M, Zhang MD, Harkany T, Hökfelt T, Rehfeld JF (2016) Nonsulfated cholecystokinins in cerebral neurons. Neuropeptides 60:37–44

Anadón R, Meléndez-Ferro M, Pérez-Costas E, Pombal MA, Rodicio MC (1998) Centrifugal fibers are the only GABAergic structures of the retina of the larval sea lamprey: an immunocytochemical study. Brain Res 782:297–302

Atoji Y, Karim MR (2014) Homology of the mesopallium in the adult chicken identified by gene expression of the neocortical marker cholecystokinin. Neurosci Lett 562:85–89

Barreiro-Iglesias A, Villar-Cerviño V, Anadón R, Rodicio MC (2008a) Development and organization of the descending serotonergic brainstem-spinal projections in the sea lamprey. J Chem Neuroanat 36:77–84

Barreiro-Iglesias A, Villar-Cerviño V, Anadón R, Rodicio MC (2008b) Descending brain-spinal cord projections in a primitive vertebrate, the lamprey: cerebrospinal fluid-contacting and dopaminergic neurons. J Comp Neurol 511:711–723

Barreiro-Iglesias A, Cornide-Petronio ME, Anadón R, Rodicio MC (2009a) Serotonin and GABA are colocalized in restricted groups of neurons in the larval sea lamprey brain: insights into the early evolution of neurotransmitter colocalization in vertebrates. J Anat 215:435–443

Barreiro-Iglesias A, Villar-Cerviño V, Anadón R, Rodicio MC (2009b) Dopamine and gamma-aminobutyric acid are colocalized in restricted groups of neurons in the sea lamprey brain: insights into the early evolution of neurotransmitter colocalization in vertebrates. J Anat 215:601–610

Barreiro-Iglesias A, Anadón R, Rodicio MC (2010a) New insights on the neuropeptide Y system in the larval lamprey brain: neuropeptide Y immunoreactive neurons, descending spinal projections and comparison with tyrosine hydroxylase and GABA immunoreactivities. Neuroscience 167:396–413

Barreiro-Iglesias A, Laramore C, Shifman MI, Anadón R, Selzer ME, Rodicio MC (2010b) The sea lamprey tyrosine hydroxylase: cDNA cloning and in situ hybridization study in the brain. Neuroscience 168:659–669

Barreiro-Iglesias A, Fernández-López B, Sobrido-Cameán D, Anadón R (2017) Organization of alpha-transducin immunoreactive system in the brain and retina of larval and young adult sea lamprey (*Petromyzon marinus*), and their relationship with other neural systems. J Comp Neurol 525:3683–3704

Barrington EJW, Dockray GJ (1970) The effect of intestinal extracts of lampreys (*Lampetra fluviatilis* and *Petromyzon marinus*) on pancreatic secretion in the rat. Gen Comp Endocrinol 14:170–177

Batten TF, Cambre ML, Moons L, Vandesande F (1990) Comparative distribution of neuropeptide-immunoreactive systems in the brain of the green molly, *Poecilia latipinna*. J Comp Neurol 302:893–919

Beinfeld MC (2001) An introduction to neuronal cholecystokinin. Peptides 22:1197–1200

Boswell T, Li Q (1998) Cholecystokinin induces Fos expression in the brain of the Japanese quail. Horm Behav 34:56–66

Bowers ME, Ressler KJ (2015) Interaction between the cholecystokinin and endogenous cannabinoid systems in cued fear expression and extinction retention. Neuropsychopharmacology 40:688–700

Brodin L, Buchanan JT, Hökfelt T, Grillner S, Rehfeld JF, Frey P et al (1988) Immunohistochemical studies of cholecystokininlike peptides and their relation to 5-HT, CGRP, and bombesin immunoreactivities in the brainstem and spinal cord of lampreys. J Comp Neurol 271:1–18

Brodin L, Rawitch A, Taylor T, Ohta Y, Ring H, Hökfelt T et al (1989) Multiple forms of pancreatic polypeptide related compounds in the lamprey CNS: partial characterization and immunohistochemical localization in the brain stem and spinal cord. J Neurosci 9:3428–3442

Buchanan JT, Brodin L, Hökfelt T, Van Dongen PA, Grillner S (1987) Survey of neuropeptide-like immunoreactivity in the lamprey spinal cord. Brain Res 408:299–302

Burgunder JM, Young WS 3rd (1988) The distribution of thalamic projection neurons containing cholecystokinin messenger RNA, using in situ hybridization histochemistry and retrograde labeling. Brain Res 464:179–189

Burgunder JM, Young WS 3rd (1989a) Ontogeny of cholecystokinin gene expression in the rat thalamus—a hybridization histochemical study. Brain Res Dev Brain Res 46:221–232

Burgunder JM, Young WS 3rd (1989b) Neurons containing cholecystokinin mRNA in the mammillary region: ontogeny and adult distribution in the rat. Cell Mol Neurobiol 9:281–294

Burgunder JM, Young WS 3rd (1990a) Cortical neurons expressing the cholecystokinin gene in the rat: distribution in the adult brain, ontogeny, and some of their projections. J Comp Neurol 300:26–46

Burgunder JM, Young WS 3rd (1990b) Ontogeny of tyrosine hydroxylase and cholecystokinin gene expression in the rat mesencephalon. Brain Res Dev Brain Res 52:85–93

Cano V, Ezquerra L, Ramos MP, Ruiz-Gayo M (2003) Characterization of the role of endogenous cholecystokinin on the activity of the paraventricular nucleus of the hypothalamus in rats. Br J Pharmacol 140:964–970

Capantini L, von Twickel A, Robertson B, Grillner S (2017) The pretectal connectome in lamprey. J Comp Neurol 525:753–772

Carrera I, Molist P, Anadón R, Rodríguez-Moldes I (2008) Development of the serotoninergic system in the central nervous system of a shark, the lesser spotted dogfish *Scyliorhinus canicula*. J Comp Neurol 511:804–831

Chandra R, Liddle RA (2007) Cholecystokinin. Curr Opin Endocrinol Diabetes Obes 14:63–67

Cho HJ, Shiotani Y, Shiosaka S, Inagaki S, Kubota Y, Kiyama H et al (1983) Ontogeny of cholecystokinin-8-containing neuron system of the rat: an immunohistochemical analysis. I. Forebrain and upper brainstem. J Comp Neurol 218:25–41

Conlon JM, Schwartz TW, Rehfeld JF (1988) Sulphated CCK-8-like peptides in the neural ganglion of the protochordate *Ciona intestinalis*. Regul Pept 20:241–250

Cornide-Petronio ME, Ruiz MS, Barreiro-Iglesias A, Rodicio MC (2011) Spontaneous regeneration of the serotonergic descending innervation in the sea lamprey after spinal cord injury. J Neurotrauma 28:2535–2540

Cornide-Petronio ME, Anadón R, Rodicio MC, Barreiro-Iglesias A (2013) The sea lamprey tryptophan hydroxylase: new insight into the evolution of the serotonergic system of vertebrates. Brain Struct Funct 218:587–593

Cornide-Petronio ME, Anadón R, Barreiro-Iglesias A, Rodicio MC (2015) Tryptophan hydroxylase and serotonin receptor 1A expression in the retina of the sea lamprey. Exp Eye Res 135:81–87

Crosby KM, Baimoukhametova DV, Bains JS, Pittman QJ (2015) Postsynaptic depolarization enhances GABA drive to dorsomedial hypothalamic neurons through somatodendritic cholecystokinin release. J Neurosci 35:13160–13170

de Arriba M-del-C, Pombal MA (2007) Afferent connections of the optic tectum in lampreys: an experimental study. Brain Behav Evol 69:37–68

De Belleroche J, Bandopadhyay R, King A, Malcolm AD, O'Brien K, Premi BP, Rashid A (1990) Regional distribution of cholecystokinin messenger RNA in rat brain during development: quantitation and correlation with cholecystokinin immunoreactivity. Neuropeptides 15:201–212

de Miguel E, Anadón R (1987) The development of retina and the optic tectum of *Petromyzon marinus*, L. A light microscopic study. J Hirnforsch 28:445–456

de Miguel E, Rodicio MC, Anadón R (1990) Organization of the visual system in larval lampreys: an HRP study. J Comp Neurol 302:529–542

Delsuc F, Philippe H, Tsagkogeorga G, Simion P, Tilak M-K, Turon X, López-Legentil S, Piette J, Lemaire P, Douzery EJP (2018) A phylogenomic framework and timescale for comparative studies of tunicates. BMC Biol 16:39

Deschenes RJ, Haun RS, Funckes CL, Dixon JE (1985) A gene encoding rat cholecystokinin. Isolation, nucleotide sequence, and promoter activity. J Biol Chem 260:1280–1286

Dockray GJ (1977) Molecular evolution of gut hormones: application of comparative studies on the regulation of digestion. Gastroenterology 72:344–358

Dockray GJ (1980) Cholecystokinins in rat cerebral cortex: identification, purification and characterization by immunochemical methods. Brain Res 188:155–165

Dupré D, Tostivint H (2014) Evolution of the gastrin–cholecystokinin gene family revealed by synteny analysis. Gen Comp Endocrinol 195:164–173

Farrell WJ, Böttger B, Ahmadi F, Finger TE (2002) Distribution of cholecystokinin, calcitonin gene-related peptide, neuropeptide Y, and galanin in the primary gustatory nuclei of the goldfish. J Comp Neurol 450:103–114

Fernández-López B, Villar-Cerviño V, Valle-Maroto SM, Barreiro-Iglesias A, Anadón R, Rodicio MC (2012) The glutamatergic neurons in the spinal cord of the sea lamprey: an in situ hybridization and immunohistochemical study. PLoS One 7:e47898

Fernández-López B, Barreiro-Iglesias A, Rodicio MC (2016) Anatomical recovery of the spinal glutamatergic system following a complete spinal cord injury in lampreys. Sci Rep 6:37786

Fernández-López B, Sobrido-Cameán D, Anadón R, Rodicio MC, Barreiro-Iglesias A (2017) Restricted co-localization of glutamate and dopamine in neurons of the adult sea lamprey brain. J Anat 231:776–784

Fox CA, Jeyapalan M, Ross LR, Jacobson CD (1991) Ontogeny of cholecystokinin-like immunoreactivity in the Brazilian opossum brain. Brain Res Dev Brain Res 64:1–18

Gasteiger E, Hoogland C, Gattiker A, Duvaud S, Wilkins MR, Appel RD, Bairoch A (2005) Protein identification and analysis tools on the ExPASy Server. In: Walker JM (ed) The proteomics protocols handbook. Humana Press, Totowa, pp 571–607

Giacobini P, Wray S (2008) Prenatal expression of cholecystokinin (CCK) in the central nervous system (CNS) of mouse. Neurosci Lett 438:96–101

Grillner S, von Twickel A, Robertson B (2018) The blueprint of the vertebrate forebrain—with special reference to the habenulae. Semin Cell Dev Biol 78:103–106

Gutièrrez-Mecinas M, Crespo C, Blasco-Ibáñez JM, Gracia-Llanes FJ, Marqués-Marí AI, Martínez-Guijarro FJ (2005) Characterization of somatostatin- and cholecystokinin-immunoreactive periglomerular cells in the rat olfactory bulb. J Comp Neurol 489:467–479

Hansen TV (2001) Cholecystokinin gene transcription: promoter elements, transcription factors and signaling pathways. Peptides 22:1201–1211

Hayes L, Zhang Z, Albert P, Zervas M, Ahn S (2011) Timing of Sonic hedgehog and Gli1 expression segregates midbrain dopamine neurons. J Comp Neurol 519:3001–3018

Hermanson O, Larhammar D, Blomqvist A (1998) Preprocholecystokinin mRNA-expressing neurons in the rat parabrachial nucleus: subnuclear localization, efferent projection, and expression of nociceptive-related intracellular signaling substances. J Comp Neurol 400:255–270

Himick BA, Peter RE (1994) CCK/gastrin-like immunoreactivity in brain and gut, and CCK suppression of feeding in goldfish. Am J Physiol 267(3 Pt 2):R841–R851

Hökfelt T, Rehfeld JF, Skirboll L, Ivemark B, Goldstein M, Markey K (1980) Evidence for coexistence of dopamine and CCK in mesolimbic neurones. Nature 285(5765):476–478

Hökfelt T, Herrera-Marschitz M, Seroogy K, Ju G, Staines WA et al (1988) Immunohistochemical studies on cholecystokinin (CCK)-immunoreactive neurons in the rat using sequence specific antisera and with special reference to the caudate nucleus and primary sensory neurons. J Chem Neuroanat 1:11–51

Holmquist AL, Dockray GJ, Rosenquist GL, Walsh JH (1979) Immunochemical characterization of cholecystokinin-like peptides in lamprey gut and brain. Gen Comp Endocrinol 37:474–481

Honda T, Wada E, Battey JF, Wank SA (1993) Differential gene expression of CCK(A) and CCK(B) receptors in the rat brain. Mol Cell Neurosci 4:143–154

Ingram SM, Krause RG 2nd, Baldino F Jr, Skeen LC, Lewis ME (1989) Neuronal localization of cholecystokinin mRNA in the rat brain by using in situ hybridization histochemistry. J Comp Neurol 287:260–272

Innis RB, Aghajanian GK (1986) Cholecystokinin-containing and nociceptive neurons in rat Edinger–Westphal nucleus. Brain Res 363:230–238

Innis RB, Corrêa FM, Uhl GR, Schneider B, Snyder SH (1979) Cholecystokinin octapeptide-like immunoreactivity: histochemical localization in rat brain. Proc Natl Acad Sci USA 76:521–525

Ivy AC, Oldberg E (1928) A hormone mechanism for gallbladder contraction and evacuation. Am J Physiol 86:559–613

Jayaraman A, Nishimori T, Dobner P, Uhl GR (1990) Cholecystokinin and neurotensin mRNAs are differentially expressed in subnuclei of the ventral tegmental area. J Comp Neurol 296:291–302

Jensen H, Rourke IJ, Møller M, Jønson L, Johnsen AH (2001) Identification and distribution of CCK-related peptides and mRNAs in the rainbow trout, *Oncorhynchus mykiss*. Biochim Biophys Acta 1517:190–201

Jiménez AJ, Mancera JM, Pombal MA, Pérez-Fígares JM, Fernández-Llebrez P (1996) Distribution of galanin-like immunoreactive elements in the brain of the adult lamprey *Lampetra fluviatilis*. J Comp Neurol 368:185–197

Johnsen AH, Jonson L, Rourke IJ, Rehfeld JF (1997) Elasmobranchs express separate cholecystokinin and gastrin genes. Proc Natl Acad Sci USA 94:10221–10226

Koyama H (2005) Organization of the sensory and motor nuclei of the glossopharyngeal and vagal nerves in lampreys. Zool Sci 22:469–476

Kubota Y, Inagaki S, Shiosaka S, Cho HJ, Tateishi K, Hashimura E et al (1983) The distribution of cholecystokinin octapeptide-like structures in the lower brain stem of the rat: an immunohistochemical analysis. Neuroscience 9:587–604

Kubota Y, Hattori R, Yui Y (1994) Three distinct subpopulations of GABAergic neurons in rat frontal agranular cortex. Brain Res 649:159–173

Kurokawa T, Suzuki T, Hashimoto H (2003) Identification of gastrin and multiple cholecystokinin genes in teleost. Peptides 24:227–235

Lannoo MJ, Hawkes R (1997) A search for primitive Purkinje cells: zebrin II expression in sea lampreys (*Petromyzon marinus*). Neurosci Lett 237:53–55

Larson LI, Rehfeld JF (1979) Localization and molecular heterogeneity of cholecystokinin in the central and peripheral nervous system. Brain Res 165:201–218

Lee MC, Schiffman SS, Pappas TN (1994) Role of neuropeptides in the regulation of feeding behavior: a review of cholecystokinin, bombesin, neuropeptide Y, and galanin. Neurosci Biobehav Rev 18:313–323

Liu CJ, Grandes P, Matute C, Cuénod M, Streit P (1989) Glutamate-like immunoreactivity revealed in rat olfactory bulb, hippocampus and cerebellum by monoclonal antibody and sensitive staining method. Histochemistry 90:427–445

Lovell PV, Mello CV (2011) Brain expression and song regulation of the cholecystokinin gene in the zebra finch (*Taeniopygia guttata*). J Comp Neurol 519:211–237

MacDonald E, Volkoff H (2009a) Cloning, distribution and effects of season and nutritional status on the expression of neuropeptide Y (NPY), cocaine and amphetamine regulated transcript (CART) and cholecystokinin (CCK) in winter flounder (*Pseudopleuronectes americanus*). Horm Behav 56:58–65

MacDonald E, Volkoff H (2009b) Neuropeptide Y (NPY), cocaine- and amphetamine-regulated transcript (CART) and cholecystokinin (CCK) in winter skate (*Raja ocellata*): cDNA cloning, tissue distribution and mRNA expression responses to fasting. Gen Comp Endocrinol 161:252–261

Maekawa F, Nakamori T, Uchimura M, Fujiwara K, Yada T, Tsukahara S et al (2007) Activation of cholecystokinin neurons in the dorsal pallium of the telencephalon is indispensable for the acquisition of chick imprinting behavior. J Neurochem 102:1645–1657

Mantyh PW, Hunt SP (1984) Evidence for cholecystokinin-like immunoreactive neurons in the rat medulla oblongata which project to the spinal cord. Brain Res 291:49–54

McClellan AD (1992) Functional regeneration and recovery of locomotor activity in spinally transected lamprey. J Exp Zool 261:274–287

McDonald AJ, Pearson JC (1989) Coexistence of GABA and peptide immunoreactivity in non-pyramidal neurons of the basolateral amygdala. Neurosci Lett 100:53–58

Meléndez-Ferro M, Pérez-Costas E, Villar-Cheda B, Abalo XM, Rodríguez-Muñoz R, Rodicio MC, Anadón R (2002) Ontogeny of gamma-aminobutyric acid-immunoreactive neuronal populations in the forebrain and midbrain of the sea lamprey. J Comp Neurol 446:360–376

Meléndez-Ferro M, Pérez-Costas E, Villar-Cheda B, Rodríguez-Muñoz R, Anadón R, Rodicio MC (2003) Ontogeny of gamma-aminobutyric acid-immunoreactive neurons in the rhombencephalon and spinal cord of the sea lamprey. J Comp Neurol 464:17–35

Mirabeau O, Joly JS (2013) Molecular evolution of peptidergic signaling systems in bilaterians. Proc Natl Acad Sci USA 110:E2028–E2037

Monigatti F, Gasteiger E, Bairoch A, Jung E (2002) The Sulfinator: predicting tyrosine sulfation sites in protein sequences. Bioinformatics 18:769–770

Monstein HJ, Thorup JU, Folkesson R, Johnsen AH, Rehfeld JF (1993) cDNA deduced procionin. Structure and expression in protochordates resemble that of procholecystokinin in mammals. FEBS Lett 331:60–64

Monti JM (2010) The structure of the dorsal raphe nucleus and its relevance to the regulation of sleep and wakefulness. Sleep Med Rev 14:307–317

Montpetit CJ, Chatalov V, Yuk J, Rasaratnam I, Youson JH (2005) Expression of neuropeptide Y family peptides in the brain and gut during stages of the life cycle of a parasitic lamprey (*Petromyzon marinus*) and a nonparasitic lamprey (*Ichthyomyzon gagei*). Ann N Y Acad Sci 1040:140–149

Moons L, Batten TFC, Vandesande F (1992) Comparative distribution of substance P (SP) and cholecystokinin (CCK) binding sites and immunoreactivity in the brain of the sea bass (*Dicentrarchus labrax*). Peptides 13:37–46

Morley JE (1982) The ascent of cholecystokinin (CCK)—from gut to brain. Life Sci 30:479–493

Murashita K, Kurokawa T, Nilsen TO, Rønnestad I (2009) Ghrelin, cholecystokinin, and peptide YY in Atlantic salmon (*Salmo salar*): molecular cloning and tissue expression. Gen Comp Endocrinol 160:223–235

Mutt V, Jorpes JE (1968) Structure of porcine cholecystokinin-pancreozymin. 1. Cleavage with thrombin and with trypsin. Eur J Biochem 6:156–162

Nachman RJ, Holman GM, Cook BJ, Haddon WF, Ling N (1986a) Leucosulfakinin-II, a blocked sulfated insect neuropeptide with homology to cholecystokinin and gastrin. Biochem Biophys Res Commun 140:357–364

Nachman RJ, Holman GM, Haddon WF, Ling N (1986b) Leucosulfakinin, a sulfated insect neuropeptide with homology to gastrin and cholecystokinin. Science 234:71–73

Negishi K, Kiyama H, Kato S, Teranishi T, Hatakenaka S, Katayama Y et al (1986) An immunohistochemical study on the river lamprey retina. Brain Res 362:389–393

Nishimura S, Bilgüvar K, Ishigame K, Sestan N, Günel M, Louvi A (2015) Functional synergy between cholecystokinin receptors CCKAR and CCKBR in mammalian brain development. PLoS One 10(4):e0124295

Ohta Y, Brodin L, Grillner S, Hökfelt T, Walsh JH (1988) Possible target neurons of the reticulospinal cholecystokinin (CCK) projection to the lamprey spinal cord: immunohistochemistry combined with intracellular staining with lucifer yellow. Brain Res 445:400–403

Panman L, Papathanou M, Laguna A, Oosterveen T, Volakakis N, Acampora D et al (2014) Sox6 and Otx2 control the specification of substantia nigra and ventral tegmental area dopamine neurons. Cell Rep 8:1018–1025

Parker D (2000) Presynaptic and interactive peptidergic modulation of reticulospinal synaptic inputs in the lamprey. J Neurophysiol 83:2497–2507

Parker D, Söderberg C, Zotova E, Shupliakov O, Langel U, Bartfai T et al (1998) Co-localized neuropeptide Y and GABA have complementary presynaptic effects on sensory synaptic transmission. Eur J Neurosci 10:2856–2870

Pérez-Fernández J, Stephenson-Jones M, Suryanarayana SM, Robertson B, Grillner S (2014) Evolutionarily conserved organization of the dopaminergic system in lamprey: SNc/VTA afferent and efferent connectivity and D2 receptor expression. J Comp Neurol 522:3775–3794

Petersen TN, Brunak S, Gunnar von Heijne G, Nielsen H (2011) SignalP 4.0: discriminating signal peptides from transmembrane regions. Nat Methods 8:785–786

Petkó M, Kovács T (1996) Distribution of cholecystokinin-8-like immunoreactivity in the frog brain and spinal cord. Acta Biol Hung 47:355–369

Peyon P, Saied H, Lin X, Peter RE (1999) Postprandial, seasonal and sexual variations in cholecystokinin gene expression in goldfish brain. Brain Res Mol Brain Res 74:190–196

Pierre J, Mahouche M, Suderevskaya EI, Repérant J, Ward R (1997) Immunocytochemical localization of dopamine and its synthetic enzymes in the central nervous system of the lamprey *Lampetra fluviatilis*. J Comp Neurol 380:119–135

Pombal MA, Megías M (2019) Development and functional organization of the cranial nerves in lampreys. Anat Rec (Hoboken) 302:512–539

Pombal MA, Puelles L (1999) Prosomeric map of the lamprey forebrain based on calretinin immunocytochemistry, Nissl stain, and ancillary markers. J Comp Neurol 414:391–422

Pombal MA, El Manira A, Grillner S (1997) Afferents of the lamprey striatum with special reference to the dopaminergic system: a combined tracing and immunohistochemical study. J Comp Neurol 386:71–91

Pombal MA, Marín O, González A (2001) Distribution of choline acetyltransferase-immunoreactive structures in the lamprey brain. J Comp Neurol 431:105–126

Pombal MA, Abalo XM, Rodicio MC, Anadón R, González A (2003) Choline acetyltransferase-immunoreactive neurons in the retina of adult and developing lampreys. Brain Res 993:154–163

Rehfeld JF (2017) Cholecystokinin—from local gut hormone to ubiquitous messenger. Front Endocrinol (Lausanne) 8:47

Rink E, Wullimann MF (2002) Connections of the ventral telencephalon and tyrosine hydroxylase distribution in the zebrafish brain (*Danio rerio*) lead to identification of an ascending dopaminergic system in a teleost. Brain Res Bull 57:385–387

Robertson B, Saitoh K, Ménard A, Grillner S (2006) Afferents of the lamprey optic tectum with special reference to the GABA input: combined tracing and immunohistochemical study. J Comp Neurol 499:106–119

Robertson B, Auclair F, Ménard A, Grillner S, Dubuc R (2007) GABA distribution in lamprey is phylogenetically conserved. J Comp Neurol 503:47–63

Rodicio MC, Pombal MA, Anadón R (1995) Early development and organization of the retinopetal system in the larval sea lamprey, *Petromyzon marinus* L. An HRP study. Anat Embryol (Berlin) 192:517–526

Rodicio MC, Villar-Cerviño V, Barreiro-Iglesias A, Anadón R (2008) Colocalization of dopamine and GABA in spinal cord neurones in the sea lamprey. Brain Res Bull 76:45–49

Roelants K, Fry BG, Norman JA, Clynen E, Schoofs L, Bossuyt F (2010) Identical skin toxins by convergent molecular adaptation in frogs. Curr Biol 20:125–130

Rourke IJ, Rehfeld JF, Møller M, Johnsen AH (1997) Characterization of the cholecystokinin and gastrin genes from the bullfrog, *Rana catesbeiana*: evolutionary conservation of primary and secondary sites of gene expression. Endocrinology 138:1719–1727

Salas CA, Yopak KE, Warrington RE, Hart NS, Potter IC, Collin SP (2015) Ontogenetic shifts in brain scaling reflect behavioral changes in the life cycle of the pouched lamprey *Geotria australis*. Front Neurosci 9:251

Satoh N, Rokhsar D, Nishikawa T (2014) Chordate evolution and the three-phylum system. Proc Biol Sci 281:20141729

Schober W (1964) Vergleichend-anatomische Untersuchungen am Gehirn der larven und adulten Tiere von *Lampetra fluviatilis* (Linne, 1758) und *Lampetra planeri* (Bloch, 1784). J Hirnforsch 7:107–209

Semmens DC, Mirabeau O, Moghul I, Pancholi MR, Wurm Y, Elphick MR (2016) Transcriptomic identification of starfish neuropeptide precursors yields new insights into neuropeptide evolution. Open Biol 6:150224

Senatorov VV, Trudeau VL, Hu B (1997) Expression of cholecystokinin messenger RNA in reciprocally-connected auditory thalamus and cortex in the rat. Neuroscience 79:915–921

Singec I, Knoth R, Ditter M, Hagemeyer CE, Rosenbrock H, Frotscher M, Volk B (2002) Synaptic vesicle protein synaptoporin is differently expressed by subpopulations of mouse hippocampal neurons. J Comp Neurol 452:139–153

Smith JJ, Kuraku S, Holt C, Sauka-Spengler T, Jiang N, Campbell MS et al (2013) Sequencing of the sea lamprey (*Petromyzon marinus*) genome provides insights into vertebrate evolution. Nat Genet 45:415–421

Söderberg C, Pieribone VA, Dahlstrand J, Brodin L, Larhammar D (1994) Neuropeptide role of both peptide YY and neuropeptide Y in vertebrates suggested by abundant expression of their mRNAs in a cyclostome brain. J Neurosci Res 37:633–640

Somogyi J, Baude A, Omori Y, Shimizu H, El Mestikawy S, Fukaya M et al (2004) GABAergic basket cells expressing cholecystokinin contain vesicular glutamate transporter type 3 (VGLUT3) in their synaptic terminals in hippocampus and isocortex of the rat. Eur J Neurosci 19:552–569

Stephenson-Jones M, Floros O, Robertson B, Grillner S (2012) Evolutionary conservation of the habenular nuclei and their circuitry controlling the dopamine and 5-hydroxytryptophan (5-HT) systems. Proc Natl Acad Sci USA 109:E164–E173

Suryanarayana SM, Robertson B, Wallén P, Grillner S (2017) The lamprey pallium provides a blueprint of the mammalian layered cortex. Curr Biol 27:3264–3277

Takahashi Y, Fukushige S, Murotsu T, Matsubara K (1986) Structure of human cholecystokinin gene and its chromosomal location. Gene 50:353–360

Tohyama M, Takatsuji K (1998) Atlas of neuroactive substances and their receptors in the rat. Oxford University Press, Oxford

Tornehave D, Hougaard DM, Larsson L (2000) Microwaving for double indirect immunofluorescence with primary antibodies from the same species and for staining of mouse tissues with mouse monoclonal antibodies. Histochem Cell Biol 113:19–23

van der Kooy D, Hunt SP, Steinbusch HW, Verhofstad AA (1981) Separate populations of cholecystokinin and 5-hydroxytryptamine-containing neuronal cells in the rat dorsal raphe, and their contribution to the ascending raphe projections. Neurosci Lett 26:25–30

van Dongen PA, Hökfelt T, Grillner S, Rehfeld JF, Verhofstad AJ (1985) A cholecystokinin-like peptide is present in 5-hydroxytryptamine neurons in the spinal cord of the lamprey. Acta Physiol Scand 125:557–560

Van Noorden S, Pearse AGE (1974) Immunoreactive polypeptide hormones in the pancreas and gut of the lamprey. Gen Comp Endocrinol 23:311–324

Vanderhaeghen JJ, Lotstra F, De Mey J, Gilles C (1980) Immunohistochemical localization of cholecystokinin- and gastrin-like peptides in the brain and hypophysis of the rat. Proc Natl Acad Sci USA 77:1190–1194

Vesselkin NP, Repérant J, Kenigfest NB, Miceli D, Ermakova TV, Rio JP (1984) An anatomical and electrophysiological study of the centrifugal visual system in the lamprey (*Lampetra fluviatilis*). Brain Res 292:41–56

Villar-Cerviño V, Abalo XM, Villar-Cheda B, Meléndez-Ferro M, Pérez-Costas E, Holstein GR et al (2006) Presence of glutamate, glycine, and gamma-aminobutyric acid in the retina of the larval sea lamprey: comparative immunohistochemical study of classical neurotransmitters in larval and postmetamorphic retinas. J Comp Neurol 499:810–827

Villar-Cerviño V, Barreiro-Iglesias A, Anadón R, Rodicio MC (2008) Distribution of glycine immunoreactivity in the brain of adult sea lamprey (*Petromyzon marinus*). Comparison with gamma-aminobutyric acid. J Comp Neurol 507:1441–1463 **(Erratum in: J Comp Neurol 508:382–384)**

Villar-Cerviño V, Barreiro-Iglesias A, Anadón R, Rodicio MC (2009) Development of glycine immunoreactivity in the brain of the sea lamprey: comparison with gamma-aminobutyric acid immunoreactivity. J Comp Neurol 512:747–767

Villar-Cerviño V, Barreiro-Iglesias A, Mazan S, Rodicio MC, Anadón R (2011) Glutamatergic neuronal populations in the forebrain of the sea lamprey, *Petromyzon marinus*: an in situ hybridization and immunocytochemical study. J Comp Neurol 519:1712–1735

Villar-Cerviño V, Barreiro-Iglesias A, Fernández-López B, Mazan S, Rodicio MC, Anadón R (2013) Glutamatergic neuronal populations in the brainstem of the sea lamprey, *Petromyzon marinus*: an in situ hybridization and immunocytochemical study. J Comp Neurol 521:522–557

Villar-Cheda B, Abalo XM, Anadón R, Rodicio MC (2006) Calbindin and calretinin immunoreactivity in the retina of adult and larval sea lamprey. Brain Res 1068:118–130

Villar-Cheda B, Abalo XM, Villar-Cerviño V, Barreiro-Iglesias A, Anadón R, Rodicio MC (2008) Late proliferation and photoreceptor differentiation in the transforming lamprey retina. Brain Res 1201:60–67

Vitale M, Vashishtha A, Linzer E, Powell DJ, Friedman JM (1991) Molecular cloning of the mouse CCK gene: expression in different brain regions and during cortical development. Nucleic Acids Res 19:169–177

Voigt MM, Uhl GR (1988) Preprocholecystokinin mRNA in rat brain: regional expression includes thalamus. Brain Res 464:247–253

Volkoff H, Canosa LF, Unniappan S, Cerdá-Reverter JM, Bernier NJ, Kelly SP, Peter RE (2005) Neuropeptides and the control of food intake in fish. Gen Comp Endocrinol 142:3–19

Wang Y, Zorio DAR, Karten HJ (2017) Heterogeneous organization and connectivity of the chicken auditory thalamus (*Gallus gallus*). J Comp Neurol 525:3044–3071

Wyeth MS, Zhang N, Houser CR (2012) Increased cholecystokinin labeling in the hippocampus of a mouse model of epilepsy maps to spines and glutamatergic terminals. Neuroscience 202:371–383

Xu X, Roby KD, Callaway EM (2010) Immunochemical characterization of inhibitory mouse cortical neurons: three chemically distinct classes of inhibitory cells. J Comp Neurol 518:389–404

Yáñez J, Anadón R (1994) Afferent and efferent connections of the habenula in the larval sea lamprey (*Petromyzon marinus* L.): an experimental study. J Comp Neurol 345:148–160

Yáñez J, Souto Y, Piñeiro L, Folgueira M, Anadón R (2017) Gustatory and general visceral centers and their connections in the brain of adult zebrafish: a carbocyanine dye tract-tracing study. J Comp Neurol 525:333–362

Yui R, Nagata Y, Fujita T (1988) Immunocytochemical studies on the islet and the gut of the arctic lamprey, *Lampetra japonica*. Arch Histol Cytol 51:109–119